



1 **Three main stages in the uplift of the Tibetan Plateau during the**
2 **Cenozoic period and its possible effects on Asian aridification: A**
3 **review**

4 **Zhixiang Wang^{1,2*} Yongjin Shen^{1,2} Zhibin Pang³**

5 ¹*State Key Laboratory of Biogeology and Environmental Geology, School of Earth Sciences,*
6 *China University of Geosciences, Wuhan 430074, China.*

7 ²*Laboratory of Critical Zone Evolution, School of Earth Sciences, China University of*
8 *Geosciences, Wuhan 430074, China*

9 ³*Shanxi Geological Survey Institute*

10

11 *Corresponding authors: wangzhi8905@126.com

12

13 **Abstract:** The Tibetan Plateau uplift and its linkages with the evolution of the Asian climate
14 during the Cenozoic are a research focus for numerous geologists. Here, a comprehensive review
15 of tectonic activities across the Tibet shows that the development of the Tibetan Plateau has
16 undergone mainly three stages of the uplift: the near-modern elevation of the central Tibet and
17 significant uplift of the northern margins (~55-35 Ma), the further uplift of the plateau margins
18 (30-20 Ma), and a rapid uplift of the plateau margins again (15-8 Ma). The first uplift of the
19 plateau during ~55-35 Ma forced the long-term westward retreat of the Paratethys Sea. The high
20 elevation of the central Tibet and/or the Himalayan would enhance rock weathering and erosion
21 contributing to lowering of atmospheric CO₂ content, resulting in global cooling. The global
22 cooling, sea retreat coupled with the topographic barrier effect of the Tibetan Plateau could have
23 caused the initial aridification in central Asia during the Eocene time. The second uplift of the
24 northern Tibet could have resulted in the onset of the East Asian winter monsoon as well as
25 intensive desertification of inland Asia, whereas the central-eastern in China became wet. The
26 further strengthening of the East Asian winter monsoon and the inland Asian aridification during
27 15-8 Ma was probably associated with the Tibetan Plateau uplift and global cooling. Therefore,
28 the uplift of the Tibetan Plateau plays a very important role in the Asian aridification.

29

30 **Keywords:** Tibetan Plateau, Asian aridification, uplift, India-Asia collision

31

32

33

34

35

36

37



1. Introduction

The collision between India and Asia during the Cenozoic period created the high Himalaya Mountains and the Tibetan Plateau, which profoundly affected the global Cenozoic climate (e.g., Garzione, 2008; Molnar et al., 2010; Raymo and Ruddiman, 1992) and the geochemical composition of the ocean as a result of input fluxes of dissolved salts from the Tibetan Plateau to the sea (e.g., Chatterjee et al., 2013; Misra and Froelich, 2012). Reconstructing the uplifting processes of the Tibetan Plateau and its relationship with crustal deformation is of wide-ranging importance to understand the lithospheric evolution, surface uplift and global climate changes.

The Tibetan Plateau covers an area of more than 2.5 million km² with an average elevation of about 5000 m. In general, the Tibetan Plateau consists of six nearly west-east stretching tectonic blocks including the Himalayan, Lhasa, Qiangtang, Songpan-Ganzi-Hoh-Xil, Kunlun-Qaidam and Qilian blocks from south to north, separated by Indus-Yarlung suture (IYS), Bangong-Nujiang suture (BNS), Jinshajiang suture (JS), Anyimaqen-Kunlun-Muttagh suture (AKMS) and South Qilian suture (SQS), respectively (Li et al., 2015; Yin and Harrison, 2000) (Fig. 1). The Lhasa and Qiangtang blocks are characterized by the main flat plateau with an average elevation of about 5000 m including several sedimentary basins. The plateau margins are a series of orogenic belts, with an average elevation ranging from 5500 to 6500 m, and sedimentary basins, such as the Qilian Mountains and Qaidam basin to the north, the Longmen Shan and Sichuan basin to the east (Fig.1). Based on seismic velocity models and wide-angle seismic profiles, the average crust thickness was interpreted as about 70-75 km under the southern Tibet, ~60-65 km under the plateau margins, and approximately 36 to 40 km beneath the Sichuan basin to the east and Tarim basin to the north (Jiang et al., 2006; Owens and Zandt, 1997; Tseng et al., 2009; Wang et al., 2007).

The timing of the initial contact and main India-Asia collision is still ambiguous with suggestions ranging from 70 to 34 Ma (Aitchison et al., 2007; DeCelles et al., 2014; Ding et al., 2005; Hu et al., 2015; Leech et al., 2005; Meng et al., 2012; Najman et al., 2010; Van Hinsbergen et al., 2012; Zhu et al., 2013), and it is probable that the main collision was not simultaneous along the entire convergent belt. Van Hinsbergen et al. (2012) proposed a two-stage India-Asia collision with phases at ~52 and 25-20 Ma based on the compilation of palaeomagnetic data from Lhasa and Tethyan Himalaya terranes. Based on the radiolarian and nannofossil biostratigraphy coupled with detrital zircon U-Pb geochronology from the Sangdanlin region in south Tibet, Hu et al. (2015) suggested that the onset of the India-Asia collision was at 59±1 Ma. Provenance analysis from upper Cretaceous-Paleocene strata in the Tethys Himalaya was proposed for the closure time of the Neo-Tethys Ocean and the India-Asia collision between 70 and 58±0.6 Ma (Cai et al., 2011; DeCelles et al., 2014). However, most of evidence based on geological, geophysical and geochemical data indicates that the main Indian subcontinent-Asia collision occurred between 55 and 50 Ma inferred by the following reasons: 1) the initiation of substantial faunal exchange of medium-to large-sized mammals during 53.3-50 Ma or a little earlier between India and Asia



76 block (e.g., Clementz et al., 2010; Clyde et al., 2003); 2) the plate motion of India decreased
77 dramatically during 55-50 Ma (e.g., Guillot et al., 2003; Shellnutt et al., 2014; van Hinsbergen et
78 al., 2011b), indicating the initial India-Asia collision (Li et al., 2015) or the slab breakoff of the
79 subducting Neo-Tethyan oceanic lithosphere (Ji et al., 2016; Zhu et al., 2015); 3) a pronounced
80 flare up in magmatic activities and the ultrahigh-pressure metamorphism around 55-50 Ma (Ding
81 et al., 2016; Donaldson et al., 2013; Guan et al., 2012; Zhu et al., 2015); 4) the provenance change
82 of the Himalayan foreland basin resulted from the first arrival of the Lhasa detritus (Green et al.,
83 2008; Najman et al., 2010; Wang et al., 2011; Zhu et al., 2005); 5) Paleomagnetic studies show
84 that the initial contact of the India-Asia collision occurred around 55-50 Ma or a little earlier (e.g.,
85 Chen et al., 2010; Huang et al., 2015; Meng et al., 2012; Najman et al., 2010; Sun et al., 2010a).
86 Tan et al. (2010) proposed a younger collision age of 43 Ma based on the paleomagnetic results
87 from the late Cretaceous red beds, lava flows and Eocene tuffs in the Lhasa block, but Najman et
88 al. (2010) suggested that the sampled volcanic tuffs were a short-term large eruption that only
89 recorded a snapshot record of the Earth magnetic field at high inclination, therefore its
90 paleomagnetic inclination should be taken caution. Therefore, we preferred an age of ~55-50 Ma
91 of initial India-Asia collision in this study.

92 After the initiation of the India-Asia collision, the Tibetan Plateau has experienced two
93 basically deformational styles. One is N-S crustal shortening and the tectonic uplift of the
94 adjoining mountains. The E-W extension and related N-S trending rifts are another deformation
95 pattern of the plateau. These two deformational styles accommodated most of India-Asia
96 convergence. However, it is still uncertain how much of the total convergence between India and
97 stable Asia after their initial collision was absorbed by the crustal shortening and E-W extension
98 since the India-Asia collision (Dupont-Nivet et al., 2010; Guillot et al., 2003; Li et al., 2015; Tan
99 et al., 2010; van Hinsbergen et al., 2011a, 2011b; Yin and Harrison, 2000). Based on the available
100 paleomagnetic data, Guillot et al. (2003) estimated a total India-Asia convergence of 3215 ± 496
101 km and ~1100 km shortening of Himalayan since 55 Ma. Dupont-Nivet et al. (2010) estimated
102 2900 ± 600 km subsequent latitudinal convergence between India and Asia, divided into 1100 ± 500
103 km within Asia and 1800 ± 700 km within India inferred from the apparent polar wander paths of
104 India and Asia. Some paleomagnetic results indicate that the Himalayan region experienced at
105 least 1500 ± 480 km of post-collisional crustal shortening and 2000 ± 550 km within Asia since the
106 collision (Sun et al., 2010a). According to the marine magnetic anomalies and the Eurasia-India
107 plate circuit, van Hinsbergen et al. (2011a) argued that the convergence was up to 3200-4000 km
108 for the India-Asia collision since 55 Ma. Recently, Li et al. (2015) concluded that ~1630 km of
109 shortening occurred across the Tibetan Plateau with more than ~1400 km accommodated by large-
110 scale thrust belts since 55 Ma based on a comprehensive review of published geological and
111 simulated data. Although the amount of India-Asia convergence accommodated by the large-scale
112 thrust belts is still uncertain, the large-scale thrust belts not only contribute to the crustal
113 shortening in central Tibet but also cause the uplift of the plateau margins (e.g., DeCelles et al.,



2002; Li et al., 2015; Tapponnier et al., 2001; Yin and Harrison, 2000).

The continued uplift of the Tibetan Plateau profoundly influenced Cenozoic global and Asian climate. Uplift of the Tibetan Plateau could have resulted in high rainfall on the front slopes of Himalayas as a result of the more intense monsoonal circulation and the orographic barrier (e.g., Thiede et al., 2004). The high Tibetan-Himalaya orogen would lead to greater rates of silicate weathering and erosion contributing to lowering of atmospheric CO₂ concentrations to force global cooling (e.g., Dupont-Nivet et al., 2008a; Garzzone, 2008; Raymo and Ruddiman, 1992). Additionally, the high Tibetan Plateau and/or only the Himalayan mountains provided the dominant heat source for the South Asian summer monsoon or orographic insulation, driving the large-scale monsoon flow and simultaneously acting as an obstacle to southward flow of cool, dry air (Boos and Kuang, 2010; Molnar et al., 2010; Wu et al., 2012). The rising Tibetan Plateau disrupted global circulation of the westerly winds, shifting the smooth flow to the diverted flow around the high plateau (e.g., Chatterjee et al., 2013). Numerous studies show that the uplift of the Himalayan-Tibetan orogen is closely related to the onset of Asian monsoon system and Asian desertification (e.g., Chatterjee et al., 2013; Guo et al., 2002; Miao et al., 2012; Zhang et al., 2007). In this paper, we synthesize the available data to propose that there are three significant stages in the uplift of the plateau and its possible effects on climatic changes in Asia.

2. Three main phases of growth of the Tibetan Plateau and Asian drying changes during the Cenozoic

Available deformational and paleoaltimetry data indicate that there were three main phases of growth of the Tibetan Plateau since the India-Asia collision. These episodes caused regionally climatic changes as well as contributing to trends in Cenozoic global cooling. The spatial and temporal evolution of the plateau growth and effects on Asian climate are divided into three episodes: the Eocene (~55-35 Ma), the middle Oligocene-early Miocene (30-20 Ma) and the middle to late Miocene (15-8 Ma).

2.1. The significant uplift of the northern margins accompanied by Asian aridification between ~55 Ma and 35 Ma

2.1.1. Asian initial aridification during ~55-35 Ma

Recent simulations show that although the high elevation of the central Tibet has already been removed, the large-scale South Asian summer monsoon circulation was unaffected by providing the high but narrow orography of the Himalaya and adjacent mountains (Boos and Kuang, 2010). These mountains produced a strong monsoon by insulating warm, moist air over continental India from the cold and dry extratropics (Boos and Kuang, 2010). Using an atmospheric general circulation model with 1.9° longitude resolution with prescribed sea surface temperature and sea ice cover to examine the effects of the plateau uplift on climate, the results were in general agreement with Boos and Kuang (2010), suggesting that the uplift of the Himalaya



150 would strengthen summer precipitation in southwestern margin of the Himalaya as well as central-
151 southern India (Zhang et al., 2012). The low oxygen isotope values with strong seasonality in
152 gastropod shells and mammal teeth from Myanmar at 40-34 Ma, and aeolian dust deposition in
153 northwest China during the Eocene time in response to the onset of desertification and winter
154 monsoon circulation in inner Asia show marked monsoon-like patterns in rainfall and wind south
155 and north of Tibetan-Himalayan orogen during the late Eocene time (Licht et al., 2014) and that
156 support the view that the Asian monsoon was probably active during the Eocene (Quan et al.,
157 2012). The similar fossil leaf trait spectra between Eocene basins in southern China and modern
158 Indonesia-Australia Monsoon suggest that the characteristics of the modern topographically
159 enhanced South Asia Monsoon had to develop in Eocene time (Spicer et al., 2016).
160 Sedimentological and numerical data shows that monsoons were not dampened by the Proto-
161 Paratethys Sea (Bougeois et al., 2018). The strong Eocene monsoons later weakened after 34 Ma
162 ago related to the global shift to icehouse climate (Licht et al., 2014).

163 The near-modern elevation of the central Tibet and further extension to the north probably
164 forced the long-term westward sea retreat from the Tarim Basin (e.g., Bosboom et al., 2014a;
165 Carrapa et al., 2015; Sun et al., 2016). The lithostratigraphic, biostratigraphic and
166 magnetostratigraphic results from the southwest Tarim Basin along the Pamir and West Kunlun
167 range show that the final sea retreat was between 47 and 40 Ma accompanied by significant
168 aridification of the Asian interior as a result of the decrease of moisture supplied from the
169 Paratethys Sea (Bosboom et al., 2014a, 2014b; Sun et al., 2016). Sedimentology, paleontology,
170 sandstone petrography and zircon U-Pb ages from the Tajik depression, 400 km to the west of the
171 Tarim basin, show that the local retreat of this part of the Paratethys Sea was at ~39 Ma, a little
172 later than the Tarim Basin (Carrapa et al., 2015). A strong anticyclonic zone at Central Asian
173 latitudes and an orographic effect from emerging Tibetan Plateau occurred during this period
174 (Bougeois et al., 2018). These results are in agreement with the northward growth of the Pamir
175 Mountains.

176 In the Xining basin at the northeastern of Tibetan Plateau, the palynological records show a
177 sudden appearance of the Pinaceae family at 38 Ma in response to the cooler and drier climate,
178 and suggest that the initiation of the continental aridification in central Asia started as early as
179 Eocene time (Dupont-Nivet et al., 2008a). Subsequent studies of the same sedimentary sequence
180 in Xining basin reveal second additional phases of aridification before the Eocene-Oligocene
181 Transition (34 Ma). The first phase at ~36.6 Ma was accompanied by a distinct decrease in gypsum
182 content relative to red mudstone and the second phase was characterized by a substantial increase
183 in clastic sedimentation rate at 34.7 Ma (Abels et al., 2011). At the Eocene-Oligocene Transition,
184 playa lake deposits in Xining basin vanished, subsequent dominated by homogenous red
185 mudstones with minor interstitial gypsum content, in response to a pronounced aridification of the
186 Xining basin (Dupont-Nivet et al., 2007).

187



188 2.1.2. Tectonic uplift of the Tibetan Plateau linked to this aridification

189 Previous studies indicate that the Lhasa and Qiangtang terranes underwent significant crustal
190 thickening and surface uplift prior to the India-Asia collision (DeCelles et al., 2002; Li et al.,
191 2015). Shortening reconstructions estimate that a ~60% crustal shortening of the Lhasa block
192 occurred during the Cretaceous and gained 3–4 km of elevation prior to the India-Asia collision
193 (Murphy et al., 1997). Balanced cross section restoration across the Qiangtang block suggests that
194 ~400 km of crustal shortening occurred prior to the India-Asia collision (Li et al., 2015; van
195 Hinsbergen et al., 2011b). The majority of intensive shortening across Central Tibet occurred
196 before the collision based on the structural restorations, and this region has been affected by only
197 minimal thrusting reactivation since the late Paleocene (Kapp et al., 2003, 2005). Therefore,
198 Central Tibet (Lhasa and Qiangtang terranes) attained at least 3 km elevation prior to India-Asia
199 collision. Since the India-Asia collision, the significant crustal thickening (~160 km) of the central
200 Tibet only occurred within about 10 Myr. The northward subduction of Greater India slab played a
201 major role in crustal thickening and uplifting (Li et al., 2015). The southward subduction of the
202 Songpan-Ganzi terrane beneath the Qiangtang block also contributed to the crustal thickening of
203 the central Tibet, as inferred from the widespread potassium-rich lavas in the northern Qiangtang
204 (Ding et al., 2007; Li et al., 2015).

205 In the Qiangtang block, stable isotope results from fluvial/lacustrine carbonate cement,
206 pedogenic carbonate and marl from the Kangtuo and Suonahu formations indicate that high
207 elevation (> 5000 m) had been established by at least the middle Oligocene (28 Ma) (Fig 2; Xu et
208 al., 2013). Stable isotopes revealed a paleoelevation of ~4.1–6.5 for the southern Tibet and 3.3 km
209 for the southeast Tibet in the Eocene, respectively (Hoke et al., 2014; Ingalls et al., 2017). The
210 low-temperature thermochronologic results from the Qiangtang and Lhasa terranes showed a rapid
211 to moderate exhumation between 85 and 45 Ma followed by low exhumation rates of <0.05 mm/yr,
212 which explained the plateau formation in central Tibet by 45 Ma (Rohrmann et al., 2011). In
213 addition, the distributions of high-K calc-alkaline andesites, dacites and rhyolites in central-
214 western Qiangtang from 46 to 38 Ma, together with the north-south trending dikes in response to
215 the onset of east-west extension in central Tibet between 47 and 38 Ma, suggested that the central
216 Tibet had already attained near-modern elevation by at least 38 Ma (Wang et al., 2008, 2010).
217 Thus, the Lhasa and Qiangtang terranes have reached near-modern elevation by at least 35 Ma.

218 The northern Tibetan Plateau had experienced significant uplift and exhumation between 55
219 and 35 Ma (Fig. 2). Low-temperature thermochronologic data shows that rocks along the major
220 thrusts—the West Qinling thrust (Clark et al., 2010; Duvall et al., 2011), Qilian Shan (He et al.,
221 2017), Tanggula thrust (Li et al., 2012), Fenghuoshan fold-thrust belt (Staisch et al., 2016),
222 Kunlun fault (Jolivet et al., 2001), Altyn Tagh thrust (Jolivet et al., 2001; Yin et al., 2002) and
223 Kashgar-Yecheng thrust (Cao et al., 2013) had undergone rapid cooling and exhumation between
224 55 and 40 Ma as a response to the initiation of India-Asia collision (Fig. 2; Locations have shown
225 on the circles and detail information can be seen at table 1). Seismic reflection profiles and



balanced cross section restoration show that the compression of the northern Qaidam basin began at 65–50 Ma, which was consistent with high accumulation rates of the foreland basin (Ji et al., 2017; Wei et al., 2013; Yin et al., 2008a) (Fig. 2).

The strong uplift of the mountains in the plateau margins during this interval would offer a large amount for clastic sediments to the adjacent basins, with peaks of influxes into the Lanzhou basin at ~58 Ma (Wang et al., 2016b), Xining basin at ~52 Ma (Dai et al., 2006), and Hoh Xil basin at ~52 Ma (Zhang et al., 2010). In the Tethyan Himalaya, emplacement of a series of undeformed granitoid bodies before 44.1 ± 1.2 Ma indicates that significant crustal thickening had occurred within 10 to 20 Myr of the initial India-Asia collision (Aikman et al., 2008). The low-temperature thermochronologic data from the Deosai plateau in the northwest Himalaya coupled with the thermal history modeling shows that the Deosai plateau underwent continuous slow exhumation rates for the past 35 Ma, thus suggesting that the high elevation had been achieved by at least 35 Ma (Fig 2; van der Beek et al., 2009). Therefore, the plateau margins have undergone significant growth shortly after the initiation of India-Asia collision, but the altitude is still disputed.

Although the Eocene global cooling that would reduce the amount of water vapor held in the atmosphere was revealed by deep-sea stable oxygen isotope (Zachos et al., 2001), we consider that the Tibetan Plateau uplift at this period played an important role in Asian aridification. First, climate models suggest that surface uplifts of the northern Tibetan Plateau had a greater contribution to the decreased annual precipitation over inland Asia mainly due to the enhanced rain shadow effect of the mountains and changes in the regional circulations (Liu et al., 2015a; Zhang et al., 2017). Second, the outward-growth of the Tibetan Plateau would force westward sea retreat of Paratethys Sea, resulting in decrease of moisture supplied into inland Asia.

2.2 The further uplift of the plateau margins and strengthened aridification in Asia between 30 and 20 Ma

2.2.1. East Asian monsoon and strengthened aridification during 30–20 Ma

The Oligocene-Miocene transition is a significant Cenozoic cooling event referred to Mi-1 with a series of paleoenvironmental changes. Benthic foraminiferal oxygen isotope from the ODP site 1218 in Pacific shows a transient ~1‰ positive excursion as a response to the expansion of Antarctic ice sheets (Zachos et al., 2001; Pälike et al., 2006), and an apparent positive excursion of benthic foraminiferal carbon isotope (Pälike et al., 2006) (Fig 3C and 3D). Sea level estimates from coastal plain coreholes in New Jersey and Delaware show an about 50 m fall of sea level between 22.3 and 23.3 Ma (Kominz et al., 2008) (Fig 3E). The CaCO_3 contents and the proportion of $> 150 \mu\text{m}$ (wt%) from ODP site 1264 and 1265 in the subtropical southeastern Atlantic Ocean show significant increases between 22.2 and 23.2 Ma as a feedback to the transient Oligocene-Miocene transition glaciations (Liebrand et al., 2016) (Fig 3F and 3G). The benthic foraminiferal accumulation rates (BFAR) at the southern Atlantic site 1090 significantly increased during



Oligocene-Miocene transition period, imply an enhanced paleoproductivity (Diester-Haass et al., 2011) (Fig 3H). Benthic foraminiferal Mg/Ca, Li/Ca and U/Ca records from ODP 926 and 929 in the equatorial Atlantic across the Oligocene-Miocene boundary reveal an enhanced organic carbon burial (Mawbey and Lear, 2013). However, the driving mechanism of this fundamental transition is still ambiguous. The relatively stable atmospheric CO₂ content may not be the reason for this climatic change (Fig 3B), and a minimum in eccentricity that results in low seasonality orbits favorable to ice-sheet expansion on Antarctica may be a dominant factor (Zachos et al., 2001) (Fig 3A).

Significantly, there were also obvious changes in Asian paleoenvironments during this interval. Based on a compilation of paleobotanical and lithological data from 125 sites over China, Sun and Wang (2005) argued that a reorganization of climate system, from latitudinal zonal pattern during the Paleogene to a Neogene pattern with arid zones restricted to northwest China, occurred around the Oligocene-Miocene boundary. This implies that the onset of the East Asia summer monsoon began around ~23 Ma. The continuous aeolian deposits during 22 to 6.2 Ma in Qin'an county (Gansu province) support the conclusion that modern East Asian monsoon already existed in the early Miocene (Fig 4; Guo et al., 2002). Subsequent studies from the Zhuanglang site at the western Chinese Loess Plateau confirmed that the loess deposits in the Loess Plateau began as early as 25 Ma and inland Asian desertification initiated or enhanced at least by the late Oligocene (Fig 4; Qiang et al., 2011). A 30 Ma stable isotope record of marine-deposited black carbon from the northern South China Sea reveals that C₄ plants gradually appeared since the early Miocene as a component of land vegetation in East Asia; and this shift in vegetation types might be related to the evolution of East Asian monsoon (Jia et al., 2003). The sporomorphs results from the Lanzhou basin during the latest Early Oligocene indicate a dominance of arboreal plants that represent a wetter environment characterized by relatively high precipitation and a warm climate, which suggests that East Asia summer monsoon has already supplied abundant rainfall to Lanzhou basin (Miao et al., 2013). Monsoonal circulation existed by the early Miocene was also supported by the presence of persistently lower pedogenic carbonate δ¹³C and higher soil respiration fluxes on the Loess Plateau and in the Himalayan foreland (Caves et al., 2016). Weathering records from the ODP 1148 in South China Sea and ODP 718 in Bay of Bengal reveal an increased intensity of chemical weathering related to onset of East Asian summer monsoon (Clift et al., 2008, 2014). The intensification of the South Asian monsoon at ~24 Ma was probably a major trigger of the stronger erosion on Greater Himalayan with removal of ~1.5 km rocks leading to a major unconformity in the Himalayan foreland basin (Clift and VanLaningham, 2010).

The aridification of Asian interior further intensified during the late Oligocene-early Miocene. In Jungger basin, the earliest eolian deposition started at 24 Ma and lasted until 8 Ma, indicating that extensive arid to semiarid regions existed in the Asian interior by 24 Ma (Sun et al., 2010b). According to the radioisotopic methods (⁴⁰Ar-³⁹Ar and U-Pb ages) to precisely date a volcanic tuff preserved in the stratigraphy from the Aertashi and Kekeya sections in the Tarim basin, in



combination with the magnetostratigraphy and lithostratigraphy, Zheng et al. (2015) concluded that the initial desertification of the Taklimakan desert was between ~26.7 Ma and 22.6 Ma as a response to a combination of widespread regional aridification and increased erosion in the surrounding mountain fronts, both of which were closely linked to the tectonic uplift of the Tibetan-Pamir Plateau and Tian Shan. A palynological record from the fluviolacustrine Jingou River section collected from the northern Tian Shan indicates a shift from a late Oligocene wet condition in central Asia to dry conditions at 23.8-23.3 Ma (Tang et al., 2011). A significant increase in aeolian sediments in Lanzhou basin occurred at ~26 Ma, which reveals that a large scale arid environment formed in the Asian interior since the late Oligocene (Zhang et al., 2014). In central Tibet, stable isotope analyses of modern and accurately dated ancient paleosol carbonate in the Nima basin reveal an arid climate and high paleoelevation (4.5-5 km) by 26 Ma (DeCelles et al., 2007). Major and trace element concentrations from the central Pacific show that the delivery of Asian dust materials significantly increased since 20 Ma in the ODP Site 1215 (Ziegler et al., 2007), which was compatible with the remarkable aridification of inland Asia.

316

2.2.2. Tectonic uplifts of the Tibet and surrounding mountains linked to this drying

This stage is characterized by relatively little tectonic active in the central Tibet and by further uplift of the plateau margins (Fig. 4; Locations that mentioned the uplift and deformation at this part have been shown on the circles and detail information can be seen table 2).

In northeastern Tibet, low-temperature thermochronologic results show that the Laji Shan (Lease et al., 2011), Ela Shan (Lu et al., 2012) and northeastern Qilian (Pan et al., 2013) underwent significant rapid cooling and exhumation between 25 and 20 Ma (Fig. 4). The unstable accumulations in the Xining basin during 25-20 Ma (Xiao et al., 2012), high accumulation rates in the Xunhua basin around 24-21 Ma (Lease et al., 2012) and sedimentary discontinuity in the Guide basin at ~21 Ma (Liu et al., 2013) have been interpreted to reflect the uplift of adjacent mountains during this period. Changes in paleocurrent and detrital zircon provenance at ~30 Ma in the Lanzhou basin at the northeast margin of the Tibetan Plateau reflect the pulsed growth of the West Qinling (Wang et al., 2016b). In the northwest Tibet, the initiation of thrusting in the West Kunlun Range began in the early Miocene (~23 Ma) (Jiang et al., 2013). The apatite fission track results indicate that the Altyn Tagh fault (Jolivet et al., 2001), the Main Pamir thrust (Sobel and Dumitru, 1997), the Southwest Tian Shan (Sobel et al., 2006), and the Northern Tian Shan (Hendrix et al., 1994) underwent rapid cooling and exhumation between 30 and 20 Ma. All of these indicate the initial activity of the thrust faults and a significant tectonic deformation of the Tibet margins during the middle Oligocene-early Miocene time (Fig. 4).

In the Himalayas, low-temperature thermochronologic results in combination with the leucogranite U-Pb and K-Ar muscovite ages show the formation of the Silving Rift as early as 23-21 Ma (Searle et al., 1999). The initial thrusting of the Main Central Thrusts occurred at approximately 23-21 Ma based on the geochronology from the dating of $^{40}\text{Ar}/^{39}\text{Ar}$ from the



Greater Himalayan paragneiss in hanging wall of the Main Central thrust (Robinson et al., 2006) and was synchronous with the South Tibetan detachment system motion (Li et al., 2015; Robinson et al., 2006). In eastern Tibet, low-temperature thermochronologic data reveals that the Longmen Shan underwent significantly cooling during 30-25 Ma (Wang et al., 2012b). Therefore, we can conclude that the plateau margins experienced intense growth between 30 and 20 Ma (Fig. 4).

The Paratethys Sea has retreated since late Eocene (Bosboom et al., 2014a), which is not the main cause of this Asian aridification. Global cooling trends and changes in CO₂ level are unlikely to account for this strengthened aridification because late Oligocene warming, as documented by the marine $\delta^{18}\text{O}$ records (Zachos et al., 2001), are not correlative with this drying changes in Asia. Therefore, we consider that the surface uplifts of the plateau margins are the dominant factor. The continuing uplift and expansion of the plateau margins would alter significantly the thermally forced circulation and enhance continental-scale winter monsoon and central Asian aridity (An et al., 2001). Climate models reveal that uplift of the northern Tibet margins have significant effects on the intensified drought in inland Asia (Liu et al., 2015a; Zhang et al., 2012). Another important factor is the Tian Shan Mountains and surrounding mountains uplift, which would reduce westerly moisture transport (Bougeois et al., 2018) and thus strengthen drying in central Asia.

2.3 The rapid uplift and erosion of the plateau margins again and Asian aridification between 15 and 8 Ma

2.3.1. Strengthened Asian winter monsoon and extensive aridification during 15-8 Ma

The middle-late Miocene time was a fundamental change in earth's climate system. A significant ~1‰ positive excursion of benthic foraminiferal $\delta^{18}\text{O}$ reflected a major expansion and permanent establishment of the East Antarctic ice sheets, and an apparent positive excursion of benthic foraminiferal $\delta^{13}\text{C}$ (Westerhold et al., 2005) (Fig 5C and 5D). Bottom waters have cooled by ~2°C and sea surface waters cooled by 6-7°C in the Southern Ocean (Holbourn et al., 2007; Shevenell et al., 2004), and cooled ~2°C of sea surface waters in the Eastern Equatorial Pacific (Rousselle et al., 2013) (Fig 5F). A 59 ± 6 m of sea level fall in northeastern Australia at ~13.9 Ma occurred due to ice growth on Antarctica (John et al., 2011). Sea level estimates from coastal plain coreholes in New Jersey and Delaware show an about 40 m fall of sea level between 14 and 11 Ma (Kominz et al., 2008) (Fig 5E). Increases in opal accumulation from 14 to 13.8 Ma from ODP U1338 in eastern equatorial Pacific indicated an enhanced siliceous productivity (Holbourn et al., 2014). During this period, the onset of a perennial sea ice cover in the Arctic Ocean probably occurred at ~13 Ma (Krylov et al., 2008), and the extinction of tundra in continental Antarctica has taken place at ~14 Ma (Lewis et al., 2008), and decrease of mass accumulation rates of silicate sediments occurred at ~15.5 Ma in South China Sea (Wan et al., 2009) (Fig 5G). Some hypotheses were tried to interpret these paleoclimatic changes, including atmospheric CO₂ drawdown (Holbourn et al., 2005; Shevenell et al., 2008) and orbitally-paced climate changes (Holbourn et al., 2007). But, the atmospheric CO₂ reconstructions still remain unclear (Fig 5B). The eccentricity



378 may be a pacemaker of middle Miocene climate evolution through the modulation of long-term
379 carbon budgets (Holbourn et al., 2007) (Fig 5A).

380 Asian paleoclimate underwent major changes during the middle to late Miocene from
381 relatively wet interval during ca. 17 to 15 Ma to a more arid one that continued to the present (Hui
382 et al., 2011; Song et al., 2014). A notable high magnetic susceptibility value interval between 16
383 and 14 Ma from Zhuanglang site at western Chinese Loess Plateau was interpreted to reflect the
384 Miocene climatic optimum (Qiang et al., 2011). Sporopollen data from the Tianshui basin at the
385 NE Tibetan Plateau indicates a dominated temperate, warm-temperate broad-leaved forest
386 between 17.1 and 14.7 Ma in response to the wet conditions (Hui et al., 2011).

387 But After ca.15 Ma, dry conditions have prevailed in the inland Asia. Palynological records
388 from the Tianshui basin (Hui et al., 2011; Liu et al., 2016), Wushan Basin in the Northeastern
389 Tibetan Plateau (Hui et al., 2017), Guyuan at the Ningxia province (Jiang and Ding, 2008),
390 western Qaidam basin (Miao et al., 2011), and northern Tian Shan (Tang et al., 2011) show that
391 the *Artemisia*, *Chenopodiaceae* (Fig 6A), *Ephedra* and *Poaceae* significantly increased and
392 remained the dominant taxa in the pollen assemblages, indicating a persistent drier condition in
393 central Asia after the middle Miocene climatic optimum. A rapid decrease of magnetic
394 susceptibility within the Neogene eolian sequences from the eastern Xorhol basin at the
395 northeastern Tibetan Plateau indicate that the aridity of Asian interior intensified after 11.5-
396 10.3 Ma period (Li et al., 2014). Carbonate content from the western Qaidam basin reveal a sharp
397 decrease since 11 Ma in response to the increase of regional aridity (Song et al., 2014) (Fig 6D).
398 Isotopic data from pedogenic and lacustrine carbonates in the northeastern Qaidam basin and
399 Xunhua basin in the northeastern Tibetan Plateau displays a positive shift of $\sim 2.5\text{‰}$ and $\sim 1.5\text{‰}$ in
400 $\delta^{18}\text{O}$ values during this period, respectively (Fig 6B), indicating that intensified aridity in central
401 Asia occurred at ~ 12 Ma (Zhuang et al., 2011; Hough et al., 2014). A similar study from the
402 southwestern Qaidam basin has shown that a $\sim 1.5\text{‰}$ positive shift in the most negative $\delta^{18}\text{O}$ values
403 of carbonate cements and pedogenic carbonates occurred at 13-12 Ma (Li et al., 2016). Another
404 similar study from the Qaidam basin show that suddenly decrease of the ostracod species diversity,
405 abrupt positive shifts of about 3.75‰ in $\delta^{18}\text{O}$ values and 5.28‰ in $\delta^{13}\text{C}$ values for ostracod
406 valves, and markedly decrease of the chemical index of weathering (CIW) occurred since 13.3 Ma
407 ago (Song et al., 2017). Multiproxies of the Sikouzi section in the Ningxia province in China
408 changed substantially after 12-11 Ma, with an increase of magnetic susceptibility, lightness and
409 total inorganic carbon and a decrease of the pollen humidity index, total organic carbon and
410 redness; these imply that the paleoclimate in central Asia became cooler and drier since 12 Ma
411 (Jiang et al., 2008). The expansion of the dry areas in western China after ca 15 Ma would supply
412 a larger amount of the dust to the Lanzhou basin (Zhang et al., 2014) and Chinese Loess Plateau
413 forming the Red Clay sediments (Xu et al., 2009). The long-term drying of inland Asia after ca 15
414 Ma led to the disappearance of late Miocene episodic lakes in the Tarim basin and shifted to the
415 currently prevailing desert environments (Liu et al., 2014). In addition, increased frequencies of



416 fire in the dry Inner Asia may be related to a continuous aridification in Asia (Miao et al., 2016).
 417 The Asian monsoon apparently changed during 14–8 Ma. Gradually increase percentages of
 418 xerophytic taxa in the Qaidam basin suggest gradual strengthening of East Asian winter monsoon
 419 and weakening of East Asian summer monsoon (Miao et al., 2011). Pollen and grain-size studies
 420 from the Sikouzi area on the east side of the Liupan Mountains also reveal a weak intensity of East
 421 Asian summer monsoon since 12 Ma ago (Jiang and Ding, 2008, 2009). Late Miocene winter
 422 monsoon intensification is evidenced in the decreased magnetic susceptibility variability of
 423 Zhuanglang Red Clay deposits (Qiang et al., 2011) (Fig 6F); which was consistent with the
 424 relatively low calcite/quartz ratios during 9.5–7.5 Ma in response to the strong East Asian winter
 425 monsoon intensity (Sun et al., 2015). Lacustrine micrite and pedogenic carbonate from the
 426 Xunhua basins at the northeastern Tibetan Plateau (Hough et al., 2011, 2014), and from the
 427 northeastern Qaidam basin (Zhuang et al., 2011) show a positive shift of ~1.5‰ and ~2.5‰ in
 428 $\delta^{18}\text{O}$ values during this period, respectively, imply an increased regional aridification and related
 429 to enhanced East Asian winter monsoon. Increased mineralogical ratios (chlorite/quartz,
 430 illite/quartz, calcite/quartz and protodolomite/quartz) from the Zhuanglang section in the western
 431 Chinese Loess Plateau indicated weak East Asian summer monsoon intensity during 18.5–9.5 Ma
 432 (Sun et al., 2015). The ratios of (illite+chlorite)/smectite and (quartz+feldspar)% from ODP site
 433 1146 in South China Sea reveal a significant increase at ~15 Ma as a result of enhanced winter
 434 monsoon (Wan et al., 2007). The CIA ($100 \times \text{Al}_2\text{O}_3 / (\text{Al}_2\text{O}_3 + \text{CaO} + \text{Na}_2\text{O} + \text{K}_2\text{O})$) from the same site
 435 1146 show a significant decrease at about 15 Ma related to decreased summer monsoon intensity
 436 (Wan et al., 2009) (Fig 6E). The illite/smectite ratios from IODP U1430 in Japan Sea show a rapid
 437 increase at ~11.8 Ma as suggestive of increased eolian input related to enhanced winter monsoon
 438 (Shen et al., 2017) (Fig 6C). A comprehensive review of numerous proxies from the South China
 439 Sea sediments reveals a strong summer monsoon during ~21–18.5 Ma, followed by an extended
 440 period of summer monsoon maximum from 18.5 to 10 Ma, then weakening (Clift et al., 2014).
 441 The South Asian summer monsoon may begin and/or strengthen during this period. The D/H
 442 ratios of pedogenic clay and the $^{18}\text{O}/^{16}\text{O}$ ratio of carbonate nodules from Siwalik sediments in
 443 India reveal a substantially strengthened Indian monsoon at ~11 Ma (Sanyal et al., 2010). But, the
 444 geophysical and geochemical data from the IODP Expedition 359 in Indian Ocean reveal an abrupt
 445 modern South Asian Monsoon onset at ~12.9 Ma (Betzler et al., 2016), with an apparent decrease
 446 content of Mn/Ca ratios (Fig 6G). This age was also reported by Gupta et al. (2015) based on the
 447 stable isotope analysis of planktonic foraminifera in the Arabian Sea and significant increase of
 448 TOC contents (Fig 6H). Recent research from ODP site 722B and 730A in the western Arabian
 449 Sea revealed a major drop in sea-surface temperature in the period of 11–10 Ma related to the
 450 establishment of monsoonal upwelling (Zhuang et al., 2017).

451

452 2.3.2. Uplifts of the plateau margins linked to this Asian drying

453 During this period, the plateau margins underwent rapid uplift again and there was the onset



454 of S-N rifting in central Tibet (Fig. 7; Locations that mentioned the uplift and deformation at this
455 part have been shown on the circles and detail information can be seen table 3).

456 In northeastern Tibet, low-temperature thermochronological and detrital zircon analyses
457 indicate that the North Qilian Shan (Zheng et al., 2010; Pan et al., 2013; Wang et al., 2016a), Jishi
458 Shan (Lease et al., 2011), Liupan Shan (Wang et al., 2017), and Haiyuan fault (Duvall et al., 2013)
459 had undergone accelerated exhumation between 14 and 10 Ma. The rapid deformation and
460 exhumation of these mountains would lead to hydrologic separation in the adjacent basins, such as
461 Xunhua and Linxia basins (Hough et al., 2011), and to a high sedimentation rate for foreland
462 basins and new detrital zircon components (Lease et al., 2012; Liu et al., 2013; Saylor et al., 2017).
463 A combination of magnetostratigraphy and cosmogenic burial ages from the fluvial deposits in
464 Gonghe basin, together with lithostratigraphic patterns and paleocurrent records, indicates that the
465 rise of the Gonghe Nan Shan became significant at ~10 Ma (Craddock et al., 2011). A clockwise
466 rotation of $25.1 \pm 4.6^\circ$ of the Guide basin took place between 17 and 11 Ma (Yan et al., 2006). A
467 magnetostratigraphic study of the Dahonggou section in the northern Qaidam basin coupled with
468 the variations in lithofacies, sedimentation rate and magnetic susceptibility reveal that the Qilian
469 Shan and the Altyn Tagh fault were synchronously tectonically active at ~12 Ma (Lu and Xiong,
470 2009). This time was consistent with the onset of molasse deposits along the Altyn Tagh fault at
471 about 13 Ma (Sun et al., 2005). In the northwestern Tibet, apatite fission track results reveal that
472 the West Kunlun range experienced rapid cooling and exhumation during 12-8 Ma, which was
473 consistent with sharply increased sedimentation rates at the southern margin of the Tarim basin
474 (Wang et al., 2003). The uplift and erosion of the Tian Shan accelerated at ~11 Ma, as constrained
475 by a two-fold increase in sedimentation rate as well as marked changes in rock magnetic
476 characteristics at this time in the Yaha section on the southern flank of the central Tian Shan
477 (Charreau et al., 2006).

478 In Himalayas, the extrusion rate of the Higher Himalayan Crystalline thrust sheet onto the
479 Lesser Himalaya sequence slowed in the middle Miocene and ceased by ca. 12 Ma (Godin et al.,
480 2006). The activity of the Main Central thrust and the South Tibetan Detachment System had
481 ceased by 13-12 Ma based on U-Pb ages of deformed pegmatites, $^{40}\text{Ar}/^{39}\text{Ar}$ hornblende ages and
482 Rb-Sr cooling ages of muscovite and biotite (Catlos et al., 2002; Daniel et al., 2003; Tobgay et al.,
483 2012). The Main Boundary thrust began active during 12-9.5 Ma inferred from the regional
484 increasing erosion in the Lesser Himalaya and rates of the foreland-basin fill (Huyghe et al., 2001;
485 Meigs et al., 1995). Thiede et al. (2009) integrated 255 apatite and zircon fission track and white
486 mica $^{40}\text{Ar}/^{39}\text{Ar}$ ages from the northwest Himalaya, and suggested that a high exhumation rate of 1-
487 2 mm/a existed since 11 Ma along the southern High Himalayan slopes. In the Tethyan Himalaya,
488 the rapid exhumation range was from 17 to 5.7 Ma in the central Himalaya and from 15 to 3 Ma in
489 the southwestern Himalaya (Liu et al., 2005; Thiede et al., 2005). A series of N-S striking rifts and
490 high-angle normal faults were documented in the Himalaya, such as the Kung Co, Thakkola,
491 Yadong-Gulu. Based on magnetostratigraphy of the Tetang Formation, the initiation of Thakkola



492 rift extension was constrained between 11 and 10 Ma (Garzione et al., 2000, 2003). The zircon and
 493 apatite (U-Th)/He ages from the footwall of the early Miocene Kung Co granite in southern Tibet
 494 suggest that initiation of normal fault slip was at ~13-12 Ma and that rapid exhumation of the
 495 footwall was between ~13 Ma and 10 Ma (Lee et al., 2011). In eastern Tibet, low-temperature
 496 thermochronological results show that southwestern Longmen Shan experienced rapid cooling at
 497 15 Ma (Cook et al., 2013), the central Longmen Shan was initially active at ~11 Ma (Kirby et al.,
 498 2002), and the northeastern part of Min Shan was at 7-4 Ma (Kirby et al., 2002). Moreover, the
 499 thermochronologic analyses from the central and southern Longmen Shan Thrust-Nappe belt reveal
 500 differential cooling across the Erwangmiao and Yingxiu-Beichuan faults during Miocene (Arne et
 501 al., 1997).

502 We cannot rule out the effects of global cooling during this period, which would reduce the
 503 amount of water vapor held in the atmosphere and thereby can cause terrestrial drying. But, the
 504 further outward-growth of the plateau margins played an important role for Asian drying. First,
 505 Miao et al.(2012) examined the evolution of Miocene climate for five separate regions in Eurasia,
 506 including Europe, High-latitude Asia, the East Asian Monsoon region, the South Asian Monsoon
 507 region, and Central Asia. The results show that the moisture evolution in Central Asia shows less
 508 similarity with other four regions, and thereby the uplift of the plateau margins could provide a
 509 possible explanation for these differences. Second, climatic proxies from the Central Asia, Japan
 510 Sea and South China Sea (Fig.6) do not show synchronously changes in response to global cooling.
 511 If we do not consider the age reliable, this may imply that regional factors, especially differential
 512 uplift of the marginal mountains on the edge of the Tibetan Plateau, played an important role for
 513 proxy changes in the context of Middle-Late Miocene global cooling.

514

515 3. Discussion

516 At least four hypotheses are proposed to interpret the Asian aridification changes: (1) the
 517 uplift of the Tibetan Plateau (e.g., Miao et al., 2012; Zheng et al., 2015); (2) the retreat of the
 518 Tethys Sea in Asia (e.g., Bosboom et al., 2014a; Ramstein et al., 1997); (3) the global cooling
 519 during the Cenozoic (e.g., Dupont-Nivet et al., 2007; Lu and Guo, 2013); and (4) the decreasing
 520 concentration of atmospheric CO₂ (e.g., Lu and Guo, 2013). Previous studies show that the retreat
 521 of the Tethys Sea occurred around 47-40 Ma. This regression was coeval with the initial
 522 aridification of the central Asia, the regional disappearance of a relatively wet perennial saline
 523 lake system, and a prominent shift to relatively more arid flora around ~41 Ma recorded in the
 524 Xining basin (Bosboom et al., 2014a; Sun et al., 2016). Therefore, some scholars suggested that
 525 the sea retreat in central Asia played an important role in the deterioration of the Asian
 526 paleoenvironment (Bosboom et al., 2014b; Ramstein et al., 1997). The global cooling is another
 527 factor for Asian desertification. The cooling would not only cause ice-sheet expansion and an
 528 increase in meridional temperature gradients leading to the southward retreat of summer monsoon,



but also would reduce the amount of water vapor held in the atmosphere leading to both additional cooling and further weakening of the East-Asian summer monsoon (e.g., Dupont-Nivet et al., 2007; Jiang and Ding, 2008; Lu and Guo, 2013). The decrease in average atmospheric CO₂ concentration would not only cause global cooling but also would shift the inter-tropical convergence zone southward, thereby reducing the monsoon precipitation accompanied by the intensification of Asian desertification (e.g., Anagnostou et al., 2016; Lu and Guo, 2013).

Although numerous elements influence evolution of East Asian climate, we consider that the three main phases of uplift of the Tibetan Plateau region played an important role in drying in Asia.

During the first pulse, the central Tibet reached the near-modern elevation and probably the Himalayas had already obtained the present-day elevation by at least 35 Ma. The high elevation in central Tibet would increase silicate weathering and erosion contributing to lowering of atmospheric CO₂, which was a major cause of global cooling (e.g., Dupont-Nivet et al., 2008a; Garzione, 2008). Global deep-sea oxygen records show a significantly positive shift in response to rapid global cooling during 50–35 Ma (Fig. 8). Reconstructions of atmospheric CO₂ concentrations based on the boron isotope composition of well preserved planktonic foraminifera show a relative decline in CO₂ concentrations through the Eocene of about 50 ppm that would be sufficient to drive the high- and low-latitude cooling during late Eocene (e.g., Anagnostou et al., 2016). The continuing uplift of the plateau, combined with a decrease of seafloor spreading rates, would result in declining atmospheric CO₂ concentrations below ~760 ppm allowed for a critical expansion of ice sheets on Antarctica (Dupont-Nivet et al., 2008a; Pearson et al., 2009). In addition, the continuing northward injection of the Pamir related to the Tibet uplift forced the long-term westward sea retreat from the Tarim basin (Carrapa et al., 2015; Sun et al., 2016). This resulted in the regional initiation of the Asian aridification induced by the decrease of moisture supplied from the Paratethys Sea (Bosboom et al., 2014b). More notably, the high Himalayas and south Tibet would lead to the formation of the south Asian monsoon by orographic insulation (Boos and Kuang, 2010) or thermal forcing (e.g., Wu et al., 2012). However, the warm and moist air from the Indian Ocean could not easily flow toward the central and northern Tibet due to the topographic barrier of the high Himalayas. Additionally, the significant uplift of the northern Tibet during this interval probably caused a relatively weak monsoon-like climate during the Eocene time, which was consistent with recent climate model simulations that the uplift of northern Tibet was critical for intensification of East Asian monsoon (Liu and Dong, 2013; Liu et al., 2015a; Tang et al., 2013).

The second pulse between 30 and 20 Ma is characterized by a further uplift of the plateau margins. However, the intense uplift of the plateau margins during this period cannot interpret the rapid warming of global climate during the Late Oligocene, which suggests that the process of silicate weathering of these elevated mountain belts and the subsequent sequestration of carbon was not sufficient in itself to counter the recorded relative rise in atmospheric CO₂ concentration (Fig. 8). Instead, this late-Oligocene climatic warming may have been partly a side-effect of a



decrease of organic carbon burial and a net addition of CO₂ to the atmosphere (e.g., Raymo and Ruddiman, 1992). Nevertheless, the uplift of the plateau margins during this interval had major regional impacts on the climate of central Asia. Climatic simulations reveal that the uplift of the northern Tibet would cause an initial formation of the East Asian monsoon as well as the desertification in central Asia (e.g., Liu and Dong, 2013; Liu et al., 2015a, 2017; Zhang et al., 2012, 2017). Moreover, the intense uplift of the northern margins would strongly strengthen the land-sea thermal contrast, thereby leading to intensification of the East Asian winter monsoon and reducing precipitation in inland Asia (Wu et al., 2012). The synchronous occurrence of the plateau uplift and intensification of the East Asian monsoon suggests that the uplift of the plateau margins was the primary mechanism for the climatic variations in central Asia during this period.

The third uplift of the plateau from 15 to 8 Ma was dominated by the uplift of the plateau margins. Although Willenbring and von Blanckenburg (2010) suggested that pulses in mountain uplift over the past 10 Ma might have been neither a direct cause nor an inevitable consequence of climate change, we consider that the Asian drying changes during this interval are primarily attributed to the rapid uplift of the Tibetan Plateau coupled with the global cooling (Fig. 8). Temperature and moisture proxy data from the five regions (Europe, high-latitude Asia, East Asian monsoon region, South Asian monsoon region, and Central Asia) suggests that the moisture evolution of central Asia was largely decoupled from adjacent regional trends during the mid-late Miocene, implying that the uplift of the Tibetan Plateau played an important role in the strengthening of aridification in central Asia (Miao et al., 2012). Climatic simulations show that the uplift of the northern Tibet would enhance the desertification of inland Asia and simultaneously strengthen the East Asian winter monsoon (Liu et al., 2015a; Tang et al., 2013). There is some evidence of a significant weaken of the East Asian summer monsoon from 14 to 11 Ma. But Chemical weathering data from ODP site 1146 and 1148 in South China Sea suggests that the summer monsoon was relatively constant and wet during 14–10 Ma (Clift et al., 2008, 2014). After 11 Ma, the further strengthening of East Asian winter monsoon was attributed to the Himalaya-Tibetan Plateau uplift and global cooling (e.g., An et al., 2001).

Although we try to establish the linkages between the uplift of the Tibetan Plateau and Asian climatic evolution, the effects between global cooling and the Tibetan Plateau uplift can still not be differentiated. Climate models did not take into account the detailed topography and other boundary conditions at each stage of the uplift (Tada et al., 2016). Additionally, there are still widely debates on paleoaltimetry of the Tibetan Plateau (Deng and Ding, 2015). Thus, more accurate evolution of the Tibetan Plateau uplift and the paleoclimatic variations in Asia should be reestablished in future.

4. Conclusion

The growth stages of the Tibetan Plateau and its margins during the Cenozoic had a series of potential effects on Asian climate. During the first stage (~55–35 Ma; Eocene), the central Tibet



has obtained near-modern elevation accompanied by the significant uplift of the northern margins. The high elevation of south Tibet would increase rates of silicate weathering, thereby leading to the drawdown of atmospheric CO₂ and contributing to global cooling. Meanwhile, the progressive northward trend in uplift of the plateau probably forced the long-term westward withdrawal of the Paratethys Sea, which contributed to the onset of regional Asian desertification by decreasing moisture supply. The global cooling and sea retreat, coupled with the topographic barrier effect of the Tibetan Plateau, were major factors in the initial aridification of central Asia.

The second uplift stage during late Oligocene and early Miocene is characterized by relatively little tectonic activity in central Tibet, but by a further uplift of the plateau margins. The uplift of northern margin of Tibet during this interval led to the onset of East Asian winter monsoon as well as the intensive desertification of inland Asia. During the third stage, from 15 to 8 Ma, the plateau margins again underwent major uplift, thereby further strengthening the Asian winter monsoon and the desertification of the inland Asia.

Acknowledgments: we are grateful to Jim Ogg for language editing that notably improved the manuscript. This work was supported by Natural Science Foundation for Distinguished Young Scholars of Hubei Province of China (2016CFA051) and the National Natural Science Foundation of China (No. 41322013).

References

- Abels H. A., Dupont-Nivet G., Xiao G., Bosboom R. and Krijgsman W.: Step-wise change of Asian interior climate preceding the Eocene–Oligocene Transition (EOT), *Palaeogeography, Palaeoclimatology, Palaeoecology*, 299, 399–412, 2011.
- Aikman A. B., Harrison T. M. and Lin D.: Evidence for Early (>44 Ma) Himalayan Crustal Thickening, Tethyan Himalaya, southeastern Tibet, *Earth and Planetary Science Letters*, 274, 14–23, 2008.
- Aitchison J. C., Ali J. R. and Davis A. M.: When and where did India and Asia collide?, *Journal of Geophysical Research*, 112, 2007.
- An Z., Kutzbach J. E., Prell W. L. and Porter S. C.: Evolution of Asian monsoons and phased uplift of the Himalaya–Tibetan plateau since Late Miocene times, *Nature*, 411, 62–66, 2001.
- Anagnostou E., John E. H., Edgar K. M., Foster G. L., Ridgwell A., Inglis G. N., Pancost R. D., Lunt D. J. and Pearson P. N.: Changing atmospheric CO concentration was the primary driver of early Cenozoic climate, *Nature*, 533, 380–384, 2016.
- Arne D., Worley B., Wilson C., Chen S. F., Foster D., Luo Z. L., Liu S. G. and Dirks P.: Differential exhumation in response to episodic thrusting along the eastern margin of the Tibetan Plateau, *Tectonophysics*, 280, 239–256, 1997.
- Betzler C., Eberli G. P., Kroon D., Wright J. D., Swart P. K., Nath B. N., Alvarezzarikian C. A., Alonsogarcía M.,



- 640 Bialik O. M. and Blättler C. L.:The abrupt onset of the modern South Asian Monsoon winds, *Sci Rep.* 6,
641 29838, 2016.
- 642 Blisniuk P. M., Hacker B. R., Glodny J., Ratschbacher L., Bi S., Wu Z., McWilliams M. O. and Calvert A.:Normal
643 faulting in central Tibet since at least 13.5 Myr ago, *Nature.* 412, 628-632, 2001.
- 644 Boos W. R. and Kuang Z.:Dominant control of the South Asian monsoon by orographic insulation versus plateau
645 heating, *Nature.* 463, 218-222, 2010.
- 646 Bosboom R., Dupont-Nivet G., Grothe A., Brinkhuis H., Villa G., Mandic O., Stoica M., Huang W., Yang W., Guo
647 Z. and Krijgsman W.:Linking Tarim Basin sea retreat (west China) and Asian aridification in the late Eocene,
648 *Basin Research.* 26, 621-640, 2014a.
- 649 Bosboom R., Dupont-Nivet G., Grothe A., Brinkhuis H., Villa G., Mandic O., Stoica M., Kouwenhoven T., Huang
650 W., Yang W. and Guo Z.:Timing, cause and impact of the late Eocene stepwise sea retreat from the Tarim
651 Basin (west China), *Palaeogeography, Palaeoclimatology, Palaeoecology.* 403, 101-118, 2014b.
- 652 Bougeois L., Dupont-Nivet G., de Rafélis M., Tindall J. C., Proust J.-N., Reichart G.-J., de Nooijer L. J., Guo Z.
653 and Ormukov C.:Asian monsoons and aridification response to Paleogene sea retreat and Neogene westerly
654 shielding indicated by seasonality in Paratethys oysters, *Earth and Planetary Science Letters.* 485, 99-110,
655 2018.
- 656 Caddick M., Bickle M., Harris N., Holland T., Horstwood M., Parrish R. and Ahmad T.:Burial and exhumation
657 history of a Lesser Himalayan schist: Recording the formation of an inverted metamorphic sequence in NW
658 India, *Earth and Planetary Science Letters.* 264, 375-390, 2007.
- 659 Cai F., Ding L. and Yue Y.:Provenance analysis of upper Cretaceous strata in the Tethys Himalaya, southern Tibet:
660 Implications for timing of India–Asia collision, *Earth and Planetary Science Letters.* 305, 195-206, 2011.
- 661 Cao K., Wang G.-C., van der Beek P., Berner M. and Zhang K.-X.:Cenozoic thermo-tectonic evolution of the
662 northeastern Pamir revealed by zircon and apatite fission-track thermochronology, *Tectonophysics.* 589, 17-
663 32, 2013.
- 664 Carrapa B., DeCelles P. G., Wang X., Clementz M. T., Mancin N., Stoica M., Kraatz B., Meng J., Abdulov S. and
665 Chen F.:Tectono-climatic implications of Eocene Paratethys regression in the Tajik basin of central Asia,
666 *Earth and Planetary Science Letters.* 424, 168-178, 2015.
- 667 Catlos E., Harrison T. M., Manning C. E., Grove M., Rai S. M., Hubbard M. S. and Upreti B.:Records of the
668 evolution of the Himalayan orogen from in situ Th–Pb ion microprobe dating of monazite: Eastern Nepal
669 and western Garhwal, *Journal of Asian Earth Sciences.* 20, 459-479, 2002.
- 670 Caves J. K., Moragne D. Y., Ibarra D. E., Bayshashov B. U., Gao Y., Jones M. M., Zhamangara A., Arzhannikova
671 A. V., Arzhannikov S. G. and Chamberlain C. P.:The Neogene de-greening of Central Asia, *Geology.* 44,
672 887-890, 2016.
- 673 Charreau J., Gilder S., Chen Y., Dominguez S., Avouac J.-P., Sen S., Jolivet M., Li Y. and Wang
674 W.:Magnetostigraphy of the Yaha section, Tarim Basin (China): 11 Ma acceleration in erosion and uplift
675 of the Tian Shan mountains, *Geology.* 34, 181-184, 2006.
- 676 Chatterjee S., Goswami A. and Scotese C. R.:The longest voyage: Tectonic, magmatic, and paleoclimatic evolution
677 of the Indian plate during its northward flight from Gondwana to Asia, *Gondwana Research.* 23, 238-267,



- 2013.
- Chen J., Huang B. and Sun L.:New constraints to the onset of the India–Asia collision: Paleomagnetic reconnaissance on the Linzizong Group in the Lhasa Block, China, *Tectonophysics*. 489, 189-209, 2010.
- Clark M. K., Farley K. A., Zheng D., Wang Z. and Duvall A. R.:Early Cenozoic faulting of the northern Tibetan Plateau margin from apatite (U–Th)/He ages, *Earth and Planetary Science Letters*. 296, 78-88, 2010.
- Clark M. K., House M. A., Royden L. H., Whipple K. X., Burchfiel B. C., Zhang X. and Tang W.:Late Cenozoic uplift of southeastern Tibet, *Geology*. 33, 525-528, 2005.
- Clementz M., Bajpai S., Ravikant V., Thewissen J. G. M., Saravanan N., Singh I. B. and Prasad V.:Early Eocene warming events and the timing of terrestrial faunal exchange between India and Asia, *Geology*. 39, 15-18, 2010.
- Clift P. D.:Controls on the erosion of Cenozoic Asia and the flux of clastic sediment to the ocean, *Earth and Planetary Science Letters*. 241, 571-580, 2006.
- Clift P. D. and VanLaningham S.:A climatic trigger for a major Oligo-Miocene unconformity in the Himalayan foreland basin, *Tectonics*. 29, n/a-n/a, 2010.
- Clift P. D., Wan S. and Blusztajn J.:Reconstructing chemical weathering, physical erosion and monsoon intensity since 25Ma in the northern South China Sea: A review of competing proxies, *Earth-Science Reviews*. 130, 86-102, 2014.
- Clift P. D., Hodges K. V., Heslop D., Hannigan R., Van Long H. and Calves G.:Correlation of Himalayan exhumation rates and Asian monsoon intensity, *Nature Geoscience*. 1, 875-880, 2008.
- Clyde W. C., Khan I. H. and Gingerich P. D.:Stratigraphic response and mammalian dispersal during initial India-Asia collision: Evidence from the Ghazij Formation, Balochistan, Pakistan, *Geology*. 31, 1097-1100, 2003.
- Cook K. L., Royden L. H., Burchfiel B. C., Lee Y. H. and Tan X.:Constraints on Cenozoic tectonics in the southwestern Longmen Shan from low-temperature thermochronology, *Lithosphere*. 5, 393-406, 2013.
- Craddock W., Kirby E. and Zhang H.:Late Miocene-Pliocene range growth in the interior of the northeastern Tibetan Plateau, *Lithosphere*. 3, 420-438, 2011.
- Dai S., Fang X., Dupont-Nivet G., Song C., Gao J., Krijgsman W., Langereis C. and Zhang W.:Magnetostatigraphy of Cenozoic sediments from the Xining Basin: Tectonic implications for the northeastern Tibetan Plateau, *Journal of Geophysical Research*. 111, 2006.
- Daniel C., Hollister L., Parrish R. t. and Grujic D.:Exhumation of the Main Central Thrust from lower crustal depths, eastern Bhutan Himalaya, *Journal of Metamorphic Geology*. 21, 317-334, 2003.
- DeCelles P. G., Robinson D. M. and Zandt G.:Implications of shortening in the Himalayan fold-thrust belt for uplift of the Tibetan Plateau, *Tectonics*. 21, 12-11-12-25, 2002.
- DeCelles P. G., Kapp P., Quade J. and Gehrels G. E.:Oligocene-Miocene Kailas basin, southwestern Tibet: Record of postcollisional upper-plate extension in the Indus-Yarlung suture zone, *Geological Society of America Bulletin*. 123, 1337-1362, 2011.
- DeCelles P. G., Kapp P., Gehrels G. E. and Ding L.:Paleocene-Eocene foreland basin evolution in the Himalaya of southern Tibet and Nepal: Implications for the age of initial India-Asia collision, *Tectonics*. 33, 824-849, 2014.



- 716 DeCelles P. G., Quade J., Kapp P., Fan M., Dettman D. L. and Ding L.:High and dry in central Tibet during the
717 Late Oligocene, *Earth and Planetary Science Letters*. 253, 389-401, 2007.
- 718 Deng T. and Ding L.:Paleoaltimetry reconstructions of the Tibetan Plateau: progress and contradictions, *National*
719 *Science Review*. 2, 417-437, 2015.
- 720 Dewane T., Stockli D., Hager C., Taylor M., Ding L., Lee J. and Wallis S. (2006). Timing of Cenozoic EW
721 Extension in the Tangra Yum Co-Kung Co Rift, south-central Tibet. *AGU Fall Meeting Abstracts*.
- 722 Diester-Haass L., Billups K. and Emeis K.:Enhanced paleoproductivity across the Oligocene/Miocene boundary as
723 evidenced by benthic foraminiferal accumulation rates, *Palaeogeography, Palaeoclimatology, Palaeoecology*.
724 302, 464-473, 2011.
- 725 Ding L., Kapp P. and Wan X.:Paleocene-Eocene record of ophiolite obduction and initial India-Asia collision,
726 south central Tibet, *Tectonics*. 24, n/a-n/a, 2005.
- 727 Ding L., Kapp P., Yue Y. and Lai Q.:Postcollisional calc-alkaline lavas and xenoliths from the southern Qiangtang
728 terrane, central Tibet, *Earth and Planetary Science Letters*. 254, 28-38, 2007.
- 729 Ding H., Zhang Z., Dong X., Tian Z., Xiang H., Mu H., Gou Z., Shui X., Li W. and Mao L.:Early Eocene (c. 50
730 Ma) collision of the Indian and Asian continents: Constraints from the North Himalayan metamorphic rocks,
731 southeastern Tibet, *Earth and Planetary Science Letters*. 435, 64-73, 2016.
- 732 Donaldson D. G., Webb A. A. G., Menold C. A., Kylander-Clark A. R. C. and Hacker B. R.:Petrochronology of
733 Himalayan ultrahigh-pressure eclogite, *Geology*. 41, 835-838, 2013.
- 734 Dupont-Nivet G., Hoorn C. and Konert M.:Tibetan uplift prior to the Eocene-Oligocene climate transition:
735 Evidence from pollen analysis of the Xining Basin, *Geology*. 36, 987-990, 2008a.
- 736 Dupont-Nivet G., Lippert P. C., Van Hinsbergen D. J. J., Meijers M. J. M. and Kapp P.:Palaeolatitude and age of
737 the Indo-Asia collision: palaeomagnetic constraints, *Geophysical Journal International*. 182, 1189-1198,
738 2010.
- 739 Dupont-Nivet G., Krijgsman W., Langereis C. G., Abels H. A., Dai S. and Fang X.:Tibetan plateau aridification
740 linked to global cooling at the Eocene-Oligocene transition, *Nature*. 445, 635-638, 2007.
- 741 Dupont-Nivet G., Dai S., Fang X., Krijgsman W., Erens V., Reitsma M. and Langereis C.:Timing and distribution
742 of tectonic rotations in the northeastern Tibetan Plateau, *Geological Society of America Special Papers*. 444,
743 73-87, 2008b.
- 744 Duvall A. R., Clark M. K., van der Pluijm B. A. and Li C.:Direct dating of Eocene reverse faulting in northeastern
745 Tibet using Ar-dating of fault clays and low-temperature thermochronometry, *Earth and Planetary Science*
746 *Letters*. 304, 520-526, 2011.
- 747 Duvall A. R., Clark M. K., Kirby E., Farley K. A., Craddock W. H., Li C. and Yuan D.-Y.:Low-temperature
748 thermochronometry along the Kunlun and Haiyuan Faults, NE Tibetan Plateau: Evidence for kinematic
749 change during late-stage orogenesis, *Tectonics*. 32, 1190-1211, 2013.
- 750 Edwards M. and Harrison T.:When did the roof collapse? Late Miocene north-south extension in the high
751 Himalaya revealed by Th-Pb monazite dating of the Khula Kangri granite, *Geology*. 25, 543-546, 1997.
- 752 Fang X., Garzzone C., Van der Voo R., Li J. and Fan M.:Flexural subsidence by 29 Ma on the NE edge of Tibet
753 from the magnetostratigraphy of Linxia Basin, China, *Earth and Planetary Science Letters*. 210, 545-560,



- 2003.
- Fang X., Zhang W., Meng Q., Gao J., Wang X., King J., Song C., Dai S. and Miao Y.:High-resolution
- magnetostratigraphy of the Neogene Huaitoutala section in the eastern Qaidam Basin on the NE Tibetan
- Plateau, Qinghai Province, China and its implication on tectonic uplift of the NE Tibetan Plateau, Earth and
- Planetary Science Letters. 258, 293-306, 2007.
- Foster G. L., Lear C. H. and Rae J. W. B.:The evolution of pCO₂, ice volume and climate during the middle
- Miocene, Earth and Planetary Science Letters. 341-344, 243-254, 2012.
- Garzione C. N.:Surface uplift of Tibet and Cenozoic global cooling, *Geology*. 36, 1003-1004, 2008.
- Garzione C. N., Dettman D. L., Quade J., DeCelles P. G. and Butler R. F.:High times on the Tibetan Plateau:
- Paleoelevation of the Thakkhola graben, Nepal, *Geology*. 28, 339-342, 2000.
- Garzione C. N., DeCelles P. G., Hodkinson D. G., Ojha T. P. and Upreti B. N.:East-west extension and Miocene
- environmental change in the southern Tibetan plateau: Thakkhola graben, central Nepal, *Geological Society*
- of America Bulletin*. 115, 3-20, 2003.
- George A. D., Marshallsea S. J., Wyrwoll K.-H., Jie C. and Yanchou L.:Miocene cooling in the northern Qilian
- Shan, northeastern margin of the Tibetan Plateau, revealed by apatite fission-track and vitrinite-reflectance
- analysis, *Geology*. 29, 939-942, 2001.
- Godin L., Grujic D., Law R. and Searle M.:Channel flow, ductile extrusion and exhumation in continental collision
- zones: an introduction, *Geological Society, London, Special Publications*. 268, 1-23, 2006.
- Green O. R., Searle M. P., Corfield R. I. and Corfield R. M.:Cretaceous-Tertiary Carbonate Platform Evolution and
- the Age of the India-Asia Collision along the Ladakh Himalaya (Northwest India), *The Journal of Geology*.
- 116, 331-353, 2008.
- Guan Q., Zhu D.-C., Zhao Z.-D., Dong G.-C., Zhang L.-L., Li X.-W., Liu M., Mo X.-X., Liu Y.-S. and Yuan H.-
- L.:Crustal thickening prior to 38Ma in southern Tibet: Evidence from lower crust-derived adakitic
- magmatism in the Gangdese Batholith, *Gondwana Research*. 21, 88-99, 2012.
- Guillot S., Garzanti E., Baratoux D., Marquer D., Mahéo G. and de Sigoyer J.:Reconstructing the total shortening
- history of the NW Himalaya, *Geochemistry, Geophysics, Geosystems*. 4, n/a-n/a, 2003.
- Guo Z., Ruddiman W. F., Hao Q., Wu H., Qiao Y., Zhu R. X., Peng S., Wei J., Yuan B. and Liu T.:Onset of Asian
- desertification by 22 Myr ago inferred from loess deposits in China, *Nature*. 416, 159-163, 2002.
- Gupta A. K., Yuvaraja A., Prakasam M., Clemens S. C. and Velu A.:Evolution of the South Asian monsoon wind
- system since the late Middle Miocene, *Palaeogeography, Palaeoclimatology, Palaeoecology*. 438, 160-167,
- 2015.
- Hager C., Stockli D., Dewane T., Gehrels G. and Ding L. (2009). Anatomy and crustal evolution of the central
- Lhasa terrane (S-Tibet) revealed by investigations in the Xainza rift. EGU General Assembly Conference
- Abstracts.
- Harrison T. M., Copeland P., Kidd W. S. F. and Lovera O. M.:Activation of the Nyainqentanghla Shear Zone:
- Implications for uplift of the southern Tibetan Plateau, *Tectonics*. 14, 658-676, 1995.
- He P., Song C., Wang Y., Chen L., Chang P., Wang Q. and Ren B.:Cenozoic exhumation in the Qilian Shan,
- northeastern Tibetan Plateau: Evidence from detrital fission track thermochronology in the Jiuquan Basin,



- 792 Journal of Geophysical Research: Solid Earth. 122, 6910-6927, 2017.
- 793 Hendrix M. S., Dumitru T. A. and Graham S. A.:Late Oligocene-early Miocene unroofing in the Chinese Tian Shan:
- 794 An early effect of the India-Asia collision, *Geology*. 22, 487-490, 1994.
- 795 Hoke G. D., Liu-Zeng J., Hren M. T., Wissink G. K. and Garzione C. N.:Stable isotopes reveal high southeast
- 796 Tibetan Plateau margin since the Paleogene, *Earth and Planetary Science Letters*. 394, 270-278, 2014.
- 797 Holbourn A., Kuhnt W., Schulz M. and Erlenkeuser H.:Impacts of orbital forcing and atmospheric carbon dioxide
- 798 on Miocene ice-sheet expansion, *Nature*. 438, 483-487, 2005.
- 799 Holbourn A., Kuhnt W., Schulz M., Flores J.-A. and Andersen N.:Orbitally-paced climate evolution during the
- 800 middle Miocene “Monterey” carbon-isotope excursion, *Earth and Planetary Science Letters*. 261, 534-550,
- 801 2007.
- 802 Holbourn A., Kuhnt W., Clemens S., Prell W. and Andersen N.:Middle to late Miocene stepwise climate cooling:
- 803 Evidence from a high-resolution deep water isotope curve spanning 8 million years, *Paleoceanography*. 28,
- 804 688-699, 2013.
- 805 Holbourn A., Kuhnt W., Lyle M., Schneider L., Romero O. and Andersen N.:Middle Miocene climate cooling
- 806 linked to intensification of eastern equatorial Pacific upwelling, *Geology*. 42, 19-22, 2014.
- 807 Hough B. G., Garzione C. N., Wang Z., Lease R. O., Burbank D. W. and Yuan D.:Stable isotope evidence for
- 808 topographic growth and basin segmentation: Implications for the evolution of the NE Tibetan Plateau,
- 809 *Geological Society of America Bulletin*. 123, 168-185, 2011.
- 810 Hu X., Garzanti E., Moore T. and Raffi I.:Direct stratigraphic dating of India-Asia collision onset at the Selandian
- 811 (middle Paleocene, 59 ± 1 Ma), *Geology*. 43, 859-862, 2015.
- 812 Huang W., Dupont - Nivet G., Lippert P. C., Hinsbergen D. J., Dekkers M. J., Waldrip R., Ganerød M., Li X., Guo
- 813 Z. and Kapp P.:What was the Paleogene latitude of the Lhasa terrane? A reassessment of the geochronology
- 814 and paleomagnetism of Linzizong volcanic rocks (Linzhou basin, Tibet), *Tectonics*. 34, 594-622, 2015.
- 815 Hui Z., Li J., Xu Q., Song C., Zhang J., Wu F. and Zhao Z.:Miocene vegetation and climatic changes reconstructed
- 816 from a sporopollen record of the Tianshui Basin, NE Tibetan Plateau, *Palaeogeography, Palaeoclimatology,*
- 817 *Palaeoecology*. 308, 373-382, 2011.
- 818 Hui Z., Li J., Song C., Chang J., Zhang J., Liu J., Liu S. and Peng T.:Vegetation and climatic changes during the
- 819 Middle Miocene in the Wushan Basin, northeastern Tibetan Plateau: Evidence from a high-resolution
- 820 palynological record, *Journal of Asian Earth Sciences*. 147, 116-127, 2017.
- 821 Huyghe P., Galy A., Mugnier J.-L. and France-Lanord C.:Propagation of the thrust system and erosion in the
- 822 Lesser Himalaya: Geochemical and sedimentological evidence, *Geology*. 29, 1007-1010, 2001.
- 823 Ingalls M., Rowley D., Olack G., Currie B., Li S., Schmidt J., Tremblay M., Polissar P., Shuster D. L., Lin D. and
- 824 Colman A.:Paleocene to Pliocene low-latitude, high-elevation basins of southern Tibet: Implications for
- 825 tectonic models of India-Asia collision, Cenozoic climate, and geochemical weathering, *GSA Bulletin*. 130,
- 826 307-330, 2017.
- 827 Ji J., Zhang K., Clift P. D., Zhuang G., Song B., Ke X. and Xu Y.:High-resolution magnetostratigraphic study of
- 828 the Paleogene-Neogene strata in the Northern Qaidam Basin: Implications for the growth of the
- 829 Northeastern Tibetan Plateau, *Gondwana Research*. 46, 141-155, 2017.



- 830 Ji W.-Q., Wu F.-Y., Chung S.-L., Wang X.-C., Liu C.-Z., Li Q.-L., Liu Z.-C., Liu X.-C. and Wang J.-G.:Eocene
831 Neo-Tethyan slab breakoff constrained by 45 Ma oceanic island basalt-type magmatism in southern Tibet,
832 Geology. 44, 283-286, 2016.
- 833 Jia G., Peng P. a., Zhao Q. and Jian Z.:Changes in terrestrial ecosystem since 30 Ma in East Asia: Stable isotope
834 evidence from black carbon in the South China Sea, Geology. 31, 1093-1096, 2003.
- 835 Jiang H. and Ding Z.:A 20 Ma pollen record of East-Asian summer monsoon evolution from Guyuan, Ningxia,
836 China, Palaeogeography, Palaeoclimatology, Palaeoecology. 265, 30-38, 2008.
- 837 Jiang H. and Ding Z.:Eolian grain-size signature of the Sikouzi lacustrine sediments (Chinese Loess Plateau):
838 Implications for Neogene evolution of the East Asian winter monsoon, Geological Society of America
839 Bulletin. 122, 843-854, 2009.
- 840 Jiang X., Li Z. X. and Li H.:Uplift of the West Kunlun Range, northern Tibetan Plateau, dominated by brittle
841 thickening of the upper crust, Geology. 41, 439-442, 2013.
- 842 Jiang H., Ji J., Gao L., Tang Z. and Ding Z.:Cooling-driven climate change at 12–11 Ma: Multiproxy records from
843 a long fluviolacustrine sequence at Guyuan, Ningxia, China, Palaeogeography, Palaeoclimatology,
844 Palaeoecology. 265, 148-158, 2008.
- 845 Jiang M., Galvé A., Hirn A., de Voogd B., Laigle M., Su H. P., Diaz J., Lépine J. C. and Wang Y. X.:Crustal
846 thickening and variations in architecture from the Qaidam basin to the Qang Tang (North–Central Tibetan
847 Plateau) from wide-angle reflection seismology, Tectonophysics. 412, 121-140, 2006.
- 848 John C. M., Karner G. D., Browning E., Leckie R. M., Mateo Z., Carson B. and Lowery C.:Timing and magnitude
849 of Miocene eustasy derived from the mixed siliciclastic-carbonate stratigraphic record of the northeastern
850 Australian margin, Earth and Planetary Science Letters. 304, 455-467, 2011.
- 851 Jolivet M., Brunel M., Seward D., Xu Z., Yang J., Roger F., Tapponnier P., Malavieille J., Arnaud N. and Wu
852 C.:Mesozoic and Cenozoic tectonics of the northern edge of the Tibetan plateau: fission-track constraints,
853 Tectonophysics. 343, 111-134, 2001.
- 854 Kali E., Leloup P., Arnaud N., Mahéo G., Liu D., Boutonnet E., Van der Woerd J., Liu X., Liu - Zeng J. and Li
855 H.:Exhumation history of the deepest central Himalayan rocks, Ama Drime range: Key pressure -
856 temperature - deformation - time constraints on orogenic models, Tectonics. 29, 2010.
- 857 Kapp P., Yin A., Harrison T. M. and Ding L.:Cretaceous-Tertiary shortening, basin development, and volcanism in
858 central Tibet, Geological Society of America Bulletin. 117, 865-878, 2005.
- 859 Kapp P., Murphy M. A., Yin A., Harrison T. M., Ding L. and Guo J.:Mesozoic and Cenozoic tectonic evolution of
860 the Shiquanhe area of western Tibet, Tectonics. 22, n/a-n/a, 2003.
- 861 Kirby E., Reiners P. W., Krol M. A., Whipple K. X., Hodges K. V., Farley K. A., Tang W. and Chen Z.:Late
862 Cenozoic evolution of the eastern margin of the Tibetan Plateau: Inferences from⁴⁰Ar/³⁹Ar and (U-Th)/He
863 thermochronology, Tectonics. 21, 2002.
- 864 Kominz M. A., Browning J. V., Miller K. G., Sugarman P. J., Mizintseva S. and Scotese C. R.:Late Cretaceous to
865 Miocene sea-level estimates from the New Jersey and Delaware coastal plain coreholes: an error analysis,
866 Basin Research. 20, 211-226, 2008.
- 867 Krylov A. A., Andreeva I. A., Vogt C., Backman J., Krupskaya V. V., Grikurov G. E., Moran K. and Shoji H.:A



- 868 shift in heavy and clay mineral provenance indicates a middle Miocene onset of a perennial sea ice cover in
- 869 the Arctic Ocean, *Paleoceanography*. 23, n/a-n/a, 2008.
- 870 Laskar J., Robutel P., Joutel F., Gastineau M., Correia A. and Levrard B.:A long-term numerical solution for the
- 871 insolation quantities of the Earth, *Astronomy & Astrophysics*. 428, 261-285, 2004.
- 872 Lease R. O., Burbank D. W., Hough B., Wang Z. and Yuan D.:Pulsed Miocene range growth in northeastern Tibet:
- 873 Insights from Xunhua Basin magnetostratigraphy and provenance, *Geological Society of America Bulletin*.
- 874 124, 657-677, 2012.
- 875 Lease R. O., Burbank D. W., Clark M. K., Farley K. A., Zheng D. and Zhang H.:Middle Miocene reorganization of
- 876 deformation along the northeastern Tibetan Plateau, *Geology*. 39, 359-362, 2011.
- 877 Lee J. and Whitehouse M. J.:Onset of mid-crustal extensional flow in southern Tibet: Evidence from U/Pb zircon
- 878 ages, *Geology*. 35, 45-48, 2007.
- 879 Lee J., Hager C., Wallis S. R., Stockli D. F., Whitehouse M. J., Aoya M. and Wang Y.:Middle to late Miocene
- 880 extremely rapid exhumation and thermal reequilibration in the Kung Co rift, southern Tibet, *Tectonics*. 30,
- 881 n/a-n/a, 2011.
- 882 Leech M., Singh S., Jain A., Klemperer S. and Manickavasagam R.:The onset of India–Asia continental collision:
- 883 Early, steep subduction required by the timing of UHP metamorphism in the western Himalaya, *Earth and*
- 884 *Planetary Science Letters*. 234, 83-97, 2005.
- 885 Lewis A. R., Marchant D. R., Ashworth A. C., Hedenas L., Hemming S. R., Johnson J. V., Leng M. J., Machlus M.
- 886 L., Newton A. E., Raine J. I., Willenbring J. K., Williams M. and Wolfe A. P.:Mid-Miocene cooling and the
- 887 extinction of tundra in continental Antarctica, *Proc Natl Acad Sci U S A*. 105, 10676-10680, 2008.
- 888 Li L., Garzzone C. N., Pullen A. and Chang H.:Early–middle Miocene topographic growth of the northern Tibetan
- 889 Plateau: Stable isotope and sedimentation evidence from the southwestern Qaidam basin, *Palaeogeography,*
- 890 *Palaeoclimatology, Palaeoecology*. 461, 201-213, 2016.
- 891 Li Y., Wang C., Zhao X., Yin A. and Ma C.:Cenozoic thrust system, basin evolution, and uplift of the Tanggula
- 892 Range in the Tuotuohe region, central Tibet, *Gondwana Research*. 22, 482-492, 2012.
- 893 Li Y., Wang C., Dai J., Xu G., Hou Y. and Li X.:Propagation of the deformation and growth of the Tibetan–
- 894 Himalayan orogen: A review, *Earth-Science Reviews*. 143, 36-61, 2015.
- 895 Li J., Yue L., Pan F., Zhang R., Guo L., Xi R. and Guo L.:Intensified aridity of the Asian interior recorded by the
- 896 magnetism of red clay in Altun Shan, NE Tibetan Plateau, *Palaeogeography, Palaeoclimatology,*
- 897 *Palaeoecology*. 411, 30-41, 2014.
- 898 Licht A., van Cappelle M., Abels H. A., Ladant J. B., Trabucho-Alexandre J., France-Lanord C., Donnadieu Y.,
- 899 Vandenbergh J., Rigaudier T., Lecuyer C., Terry D., Jr., Adriaens R., Boura A., Guo Z., Soe A. N., Quade J.,
- 900 Dupont-Nivet G. and Jaeger J. J.:Asian monsoons in a late Eocene greenhouse world, *Nature*. 513, 501-506,
- 901 2014.
- 902 Liebrand D., Beddow H. M., Lourens L. J., Pälike H., Raffi I., Bohaty S. M., Hilgen F. J., Saes M. J. M., Wilson P.
- 903 A., van Dijk A. E., Hodell D. A., Kroon D., Huck C. E. and Batenburg S. J.:Cyclostratigraphy and
- 904 eccentricity tuning of the early Oligocene through early Miocene (30.1–17.1 Ma): *Cibicides mundulus* stable
- 905 oxygen and carbon isotope records from Walvis Ridge Site 1264, *Earth and Planetary Science Letters*. 450,



- 906 392-405, 2016.
- 907 Liu X. and Dong B.:Influence of the Tibetan Plateau uplift on the Asian monsoon-arid environment evolution,
- 908 Chinese Science Bulletin. 58, 4277-4291, 2013.
- 909 Liu D., Li D., Yang W., Wang X. and Zhang J.:Evidence from fission track ages for the tectonic uplift of the
- 910 Himalayan orogen during Late Cenozoic, Earth Sci. J. China Univ. Geosci. 30, 147-152, 2005.
- 911 Liu X., Sun H., Miao Y., Dong B. and Yin Z.-Y.:Impacts of uplift of northern Tibetan Plateau and formation of
- 912 Asian inland deserts on regional climate and environment, Quaternary Science Reviews. 116, 1-14, 2015a.
- 913 Liu X., Dong B., Yin Z. Y., Smith R. S. and Guo Q.:Continental drift and plateau uplift control origination and
- 914 evolution of Asian and Australian monsoons, Sci Rep. 7, 40344, 2017.
- 915 Liu S., Zhang G., Pan F., Zhang H., Wang P., Wang K. and Wang Y.:Timing of Xunhua and Guide basin
- 916 development and growth of the northeastern Tibetan Plateau, China, Basin Research. 25, 74-96, 2013.
- 917 Liu D., Li H., Sun Z., Pan J., Wang M., Wang H. and Marie L.:AFT dating constrains the Cenozoic uplift of the
- 918 Qimen Tagh Mountains, Northeast Tibetan Plateau, comparison with LA-ICPMS Zircon U–Pb ages,
- 919 Gondwana Research. 41, 438-450, 2015b.
- 920 Liu J., Li J. J., Song C. H., Yu H., Peng T. J., Hui Z. C. and Ye X. Y.:Palynological evidence for late Miocene
- 921 stepwise aridification on the northeastern Tibetan Plateau, Climate of the Past. 12, 1473-1484, 2016.
- 922 Liu W., Liu Z., An Z., Sun J., Chang H., Wang N., Dong J. and Wang H.:Late Miocene episodic lakes in the arid
- 923 Tarim Basin, western China, Proceedings of the National Academy of Sciences. 111, 16292-16296, 2014.
- 924 Lu H. and Xiong S.:Magnetostatigraphy of the Dahonggou section, northern Qaidam Basin and its bearing on
- 925 Cenozoic tectonic evolution of the Qilian Shan and Altyn Tagh Fault, Earth and Planetary Science Letters.
- 926 288, 539-550, 2009.
- 927 Lu H. and Guo Z.:Evolution of the monsoon and dry climate in East Asia during late Cenozoic: A review, Science
- 928 China Earth Sciences. 57, 70-79, 2013.
- 929 Lu H., Wang E., Shi X. and Meng K.:Cenozoic tectonic evolution of the Elashan range and its surroundings,
- 930 northern Tibetan Plateau as constrained by paleomagnetism and apatite fission track analyses,
- 931 Tectonophysics. 580, 150-161, 2012.
- 932 Lu H., Wang X., An Z., Miao X., Zhu R., Ma H., LI Z., Tan H. and Wang X.:Geomorphologic evidence of phased
- 933 uplift of the northeastern Qinghai-Tibet Plateau since 14 million years ago, Science in China (series D). 47,
- 934 822-833, 2004.
- 935 Mawbey E. M. and Lear C. H.:Carbon cycle feedbacks during the Oligocene-Miocene transient glaciation,
- 936 Geology. 41, 963-966, 2013.
- 937 Meigs A. J., Burbank D. W. and Beck R. A.:Middle-late Miocene (> 10 Ma) formation of the Main Boundary
- 938 thrust in the western Himalaya, Geology. 23, 423-426, 1995.
- 939 Meng J., Wang C., Zhao X., Coe R., Li Y. and Finn D.:India-Asia collision was at 24 degrees N and 50 Ma:
- 940 palaeomagnetic proof from southernmost Asia, Sci Rep. 2, 925, 2012.
- 941 Miao Y., Herrmann M., Wu F., Yan X. and Yang S.:What controlled Mid–Late Miocene long-term aridification in
- 942 Central Asia? — Global cooling or Tibetan Plateau uplift: A review, Earth-Science Reviews. 112, 155-172,
- 943 2012.



- 944 Miao Y., Wu F., Herrmann M., Yan X. and Meng Q.:Late early Oligocene East Asian summer monsoon in the NE
945 Tibetan Plateau: Evidence from a palynological record from the Lanzhou Basin, China, *Journal of Asian*
946 *Earth Sciences*. 75, 46-57, 2013.
- 947 Miao Y., Fang X., Herrmann M., Wu F., Zhang Y. and Liu D.:Miocene pollen record of KC-1 core in the Qaidam
948 Basin, NE Tibetan Plateau and implications for evolution of the East Asian monsoon, *Palaeogeography,*
949 *Palaeoclimatology, Palaeoecology*. 299, 30-38, 2011.
- 950 Miao Y., Fang X., Song C., Yan X., Zhang P., Meng Q., Li F., Wu F., Yang S., Kang S. and Wang Y.:Late Cenozoic
951 fire enhancement response to aridification in mid-latitude Asia: Evidence from microcharcoal records,
952 *Quaternary Science Reviews*. 139, 53-66, 2016.
- 953 Misra S. and Froelich P. N.:Lithium isotope history of Cenozoic seawater: changes in silicate weathering and
954 reverse weathering, *Science*. 335, 818-823, 2012.
- 955 Molnar P., Boos W. R. and Battisti D. S.:Orographic Controls on Climate and Paleoclimate of Asia: Thermal and
956 Mechanical Roles for the Tibetan Plateau, *Annual Review of Earth and Planetary Sciences*. 38, 77-102, 2010.
- 957 Murphy M. A., Yin A., Harrison T. M., Dürr S. B., Z C., Ryerson F. J., Kidd W. S. F., X W. and X Z.:Did the Indo-
958 Asian collision alone create the Tibetan plateau?, *Geology*. 25, 719-722, 1997.
- 959 Najman Y., Appel E., Boudagher-Fadel M., Bown P., Carter A., Garzanti E., Godin L., Han J., Liebke U., Oliver G.,
960 Parrish R. and Vezzoli G.:Timing of India-Asia collision: Geological, biostratigraphic, and palaeomagnetic
961 constraints, *Journal of Geophysical Research*. 115, 2010.
- 962 Owens T. J. and Zandt G.:Implications of crustal property variations for models of Tibetan plateau evolution,
963 *Nature*. 387, 37-43, 1997.
- 964 Pagani M., Arthur M. A. and Freeman K. H.:Miocene evolution of atmospheric carbon dioxide, *Paleoceanography*.
965 14, 273-292, 1999a.
- 966 Pagani M., Freeman K. H. and Arthur M. A.:Late Miocene Atmospheric CO₂ Concentrations and the Expansion of
967 C₄ Grasses, *Science*. 285, 876, 1999b.
- 968 Pagani M., Zachos J. C., Freeman K. H., Tiplle B. and Bohaty S.:Marked decline in atmospheric carbon dioxide
969 concentrations during the Paleogene, *Science*. 309, 600-603, 2005.
- 970 Pälike H., Norris R. D., Herrle J. O., Wilson P. A., Coxall H. K., Lear C. H., Shackleton N. J., Tripathi A. K. and
971 Wade B. S.:The heartbeat of the Oligocene climate system, *science*. 314, 1894-1898, 2006.
- 972 Pan B., Li Q., Hu X., Geng H., Liu Z., Jiang S. and Yuan W.:Cretaceous and Cenozoic cooling history of the
973 eastern Qilian Shan, north-eastern margin of the Tibetan Plateau: evidence from apatite fission-track analysis,
974 *Terra Nova*. 25, 431-438, 2013.
- 975 Pearson P. N., Foster G. L. and Wade B. S.:Atmospheric carbon dioxide through the Eocene-Oligocene climate
976 transition, *Nature*. 461, 1110-1113, 2009.
- 977 Qiang X., An Z., Song Y., Chang H., Sun Y., Liu W., Ao H., Dong J., Fu C., Wu F., Lu F., Cai Y., Zhou W., Cao J.,
978 Xu X. and Ai L.:New eolian red clay sequence on the western Chinese Loess Plateau linked to onset of
979 Asian desertification about 25 Ma ago, *Science China Earth Sciences*. 54, 136-144, 2011.
- 980 Quan C., Liu Y.-S. and Utescher T.:Eocene monsoon prevalence over China: A paleobotanical perspective,
981 *Palaeogeography, Palaeoclimatology, Palaeoecology*. 365-366, 302-311, 2012.



- 982 Ramstein G., Fluteau F., Besse J. and Joussaume S.:Effect of orogeny, plate motion and land–sea distribution on
- 983 Eurasian climate change over the past 30 million years, *Nature*. 386, 788-795, 1997.
- 984 Raymo M. and Ruddiman W. F.:Tectonic forcing of late Cenozoic climate, *Nature*. 359, 117-122, 1992.
- 985 Robinson D. M., DeCelles P. G. and Copeland P.:Tectonic evolution of the Himalayan thrust belt in western Nepal:
- 986 Implications for channel flow models, *Geological Society of America Bulletin*. 118, 865-885, 2006.
- 987 Rohrmann A., Kapp P., Carrapa B., Reiners P. W., Gynn J., Ding L. and Heizler M.:Thermochronologic evidence
- 988 for plateau formation in central Tibet by 45 Ma, *Geology*. 40, 187-190, 2011.
- 989 Rousselle G., Beltran C., Sicre M.-A., Raffi I. and De Rafélis M.:Changes in sea-surface conditions in the
- 990 Equatorial Pacific during the middle Miocene–Pliocene as inferred from coccolith geochemistry, *Earth and*
- 991 *Planetary Science Letters*. 361, 412-421, 2013.
- 992 Sanyal P., Sarkar A., Bhattacharya S. K., Kumar R., Ghosh S. K. and Agrawal S.:Intensification of monsoon,
- 993 microclimate and asynchronous C4 appearance: Isotopic evidence from the Indian Siwalik sediments,
- 994 *Palaeogeography, Palaeoclimatology, Palaeoecology*. 296, 165-173, 2010.
- 995 Saylor J. E., Jordan J. C., Sundell K. E., Wang X., Wang S. and Deng T.:Topographic growth of the Jishi Shan and
- 996 its impact on basin and hydrology evolution, NE Tibetan Plateau, *Basin Research*. 10.1111/bre.122642017.
- 997 Searle M., Noble S., Hurford A. J. and Rex D.:Age of crustal melting, emplacement and exhumation history of the
- 998 Shivaling leucogranite, Garhwal Himalaya, *Geological Magazine*. 136, 513-525, 1999.
- 999 Shellnutt J. G., Lee T.-Y., Brookfield M. E. and Chung S.-L.:Correlation between magmatism of the Ladakh
- 1000 Batholith and plate convergence rates during the India–Eurasia collision, *Gondwana Research*. 26, 1051-
- 1001 1059, 2014.
- 1002 Shen X., Wan S., France-Lanord C., Clift P. D., Tada R., Révillon S., Shi X., Zhao D., Liu Y., Yin X., Song Z. and
- 1003 Li A.:History of Asian eolian input to the Sea of Japan since 15 Ma: Links to Tibetan uplift or global
- 1004 cooling?, *Earth and Planetary Science Letters*. 474, 296-308, 2017.
- 1005 Shevenell A. E., Kennett J. P. and Lea D. W.:Middle Miocene Southern Ocean cooling and Antarctic cryosphere
- 1006 expansion, *Science*. 305, 1766-1770, 2004.
- 1007 Shevenell A. E., Kennett J. P. and Lea D. W.:Middle Miocene ice sheet dynamics, deep-sea temperatures, and
- 1008 carbon cycling: A Southern Ocean perspective, *Geochemistry, Geophysics, Geosystems*. 9, n/a-n/a, 2008.
- 1009 Sobel E. and Dumitru T.:Exhumation of the margins of the western Tarim basin during the Himalayan orogeny, *J.*
- 1010 *Geophys. Res.* 102, 5043-5064, 1997.
- 1011 Sobel E., Chen J. and Heermance R.:Late Oligocene–Early Miocene initiation of shortening in the Southwestern
- 1012 Chinese Tian Shan: Implications for Neogene shortening rate variations, *Earth and Planetary Science Letters*.
- 1013 247, 70-81, 2006.
- 1014 Song B., Ji J., Wang C., Xu Y. and Zhang U. K.:Intensified aridity in the Qaidam Basin during the middle Miocene:
- 1015 con, *Canadian Journal of Earth Sciences*. 54, 2017.
- 1016 Song C., Hu S., Han W., Zhang T., Fang X., Gao J. and Wu F.:Middle Miocene to earliest Pliocene
- 1017 sedimentological and geochemical records of climate change in the western Qaidam Basin on the NE
- 1018 Tibetan Plateau, *Palaeogeography, Palaeoclimatology, Palaeoecology*. 395, 67-76, 2014.
- 1019 Spicer R. A., Yang J., Herman A. B., Kodrul T., Maslova N., Spicer T. E., Aleksandrova G. and Jin J.:Asian Eocene



- 1020 monsoons as revealed by leaf architectural signatures, *Earth and Planetary Science Letters*. 449, 61-68, 2016.
- 1021 Staisch L. M., Niemi N. A., Clark M. K. and Hong C.:Eocene - late Oligocene history of crustal shortening within
- 1022 the Hoh Xil Basin and implications for the uplift history of the northern Tibetan Plateau, *Tectonics*.
- 1023 10.1002/2015tc003972n/a-n/a, 2016.
- 1024 Sun X. and Wang P.:How old is the Asian monsoon system?—Palaeobotanical records from China,
- 1025 Palaeogeography, Palaeoclimatology, Palaeoecology. 222, 181-222, 2005.
- 1026 Sun J., Zhu R. and An Z.:Tectonic uplift in the northern Tibetan Plateau since 13.7 Ma ago inferred from molasse
- 1027 deposits along the Altyn Tagh Fault, *Earth and Planetary Science Letters*. 235, 641-653, 2005.
- 1028 Sun Z., Jiang W., Li H., Pei J. and Zhu Z.:New paleomagnetic results of Paleocene volcanic rocks from the Lhasa
- 1029 block: Tectonic implications for the collision of India and Asia, *Tectonophysics*. 490, 257-266, 2010a.
- 1030 Sun J., Windley B. F., Zhang Z., Fu B. and Li S.:Diachronous seawater retreat from the southwestern margin of the
- 1031 Tarim Basin in the late Eocene, *Journal of Asian Earth Sciences*. 116, 222-231, 2016.
- 1032 Sun Y., Ma L., Bloemendal J., Clemens S., Qiang X. and An Z.:Miocene climate change on the Chinese Loess
- 1033 Plateau: Possible links to the growth of the northern Tibetan Plateau and global cooling, *Geochemistry,*
- 1034 *Geophysics, Geosystems*. 16, 2097-2108, 2015.
- 1035 Sun J., Ye J., Wu W., Ni X., Bi S., Zhang Z., Liu W. and Meng J.:Late Oligocene-Miocene mid-latitude
- 1036 aridification and wind patterns in the Asian interior, *Geology*. 38, 515-518, 2010b.
- 1037 Tada R., Zheng H. and Clift P. D.:Evolution and variability of the Asian monsoon and its potential linkage with
- 1038 uplift of the Himalaya and Tibetan Plateau, *Progress in Earth and Planetary Science*. 3, 2016.
- 1039 Tan X., Gilder S., Kodama K. P., Jiang W., Han Y., Zhang H., Xu H. and Zhou D.:New paleomagnetic results from
- 1040 the Lhasa block: Revised estimation of latitudinal shortening across Tibet and implications for dating the
- 1041 India–Asia collision, *Earth and Planetary Science Letters*. 293, 396-404, 2010.
- 1042 Tang H., Micheels A., Eronen J. T., Ahrens B. and Fortelius M.:Asynchronous responses of East Asian and Indian
- 1043 summer monsoons to mountain uplift shown by regional climate modelling experiments, *Climate Dynamics*.
- 1044 40, 1531-1549, 2013.
- 1045 Tang Z., Ding Z., White P. D., Dong X., Ji J., Jiang H., Luo P. and Wang X.:Late Cenozoic central Asian drying
- 1046 inferred from a palynological record from the northern Tian Shan, *Earth and Planetary Science Letters*. 302,
- 1047 439-447, 2011.
- 1048 Tapponnier P., Zhiqin X., Roger F., Meyer B., Arnaud N., Wittlinger G. and Jingsui Y.:Oblique stepwise rise and
- 1049 growth of the Tibet Plateau, *science*. 294, 1671-1677, 2001.
- 1050 Thiede R. C., Ehlers T. A., Bookhagen B. and Strecker M. R.:Erosional variability along the northwest Himalaya,
- 1051 *Journal of Geophysical Research*. 114, 2009.
- 1052 Thiede R. C., Bookhagen B., Arrowsmith J. R., Sobel E. R. and Strecker M. R.:Climatic control on rapid
- 1053 exhumation along the Southern Himalayan Front, *Earth and Planetary Science Letters*. 222, 791-806, 2004.
- 1054 Thiede R. C., Arrowsmith J. R., Bookhagen B., McWilliams M. O., Sobel E. R. and Strecker M. R.:From
- 1055 tectonically to erosionally controlled development of the Himalayan orogen, *Geology*. 33, 689-692, 2005.
- 1056 Tobgay T., McQuarrie N., Long S., Kohn M. J. and Corrie S. L.:The age and rate of displacement along the Main
- 1057 Central Thrust in the western Bhutan Himalaya, *Earth and Planetary Science Letters*. 319-320, 146-158,



- 2012.
- Tripathi A. K., Roberts C. D. and Eagle R. A.:Coupling of CO₂ and ice sheet stability over major climate transitions of the last 20 million years, *Science*. 326, 1394-1397, 2009.
- Tseng T.-L., Chen W.-P. and Nowack R. L.:Northward thinning of Tibetan crust revealed by virtual seismic profiles, *Geophysical Research Letters*. 36, 2009.
- van der Beek P., Van Melle J., Guillot S., Pêcher A., Reiners P. W., Nicolescu S. and Latif M.:Eocene Tibetan plateau remnants preserved in the northwest Himalaya, *Nature Geoscience*. 2, 364-368, 2009.
- van Hinsbergen D. J. J., Steinberger B., Doubrovine P. V. and Gassmöller R.:Acceleration and deceleration of India-Asia convergence since the Cretaceous: Roles of mantle plumes and continental collision, *Journal of Geophysical Research*. 116, 2011a.
- van Hinsbergen D. J. J., Kapp P., Dupont-Nivet G., Lippert P. C., DeCelles P. G. and Torsvik T. H.:Restoration of Cenozoic deformation in Asia and the size of Greater India, *Tectonics*. 30, n/a-n/a, 2011b.
- Van Hinsbergen D. J., Lippert P. C., Dupont-Nivet G., McQuarrie N., Doubrovine P. V., Spakman W. and Torsvik T. H.:Greater India Basin hypothesis and a two-stage Cenozoic collision between India and Asia, *Proceedings of the National Academy of Sciences*. 109, 7659-7664, 2012.
- Vannay J. C., Grasemann B., Rahn M., Frank W., Carter A., Baudraz V. and Cosca M.:Miocene to Holocene exhumation of metamorphic crustal wedges in the NW Himalaya: Evidence for tectonic extrusion coupled to fluvial erosion, *Tectonics*. 23, 2004.
- Viskupic K., Hodges K. V. and Bowring S. A.:Timescales of melt generation and the thermal evolution of the Himalayan metamorphic core, Everest region, eastern Nepal, *Contributions to Mineralogy and Petrology*. 149, 1-21, 2005.
- Walker J., Martin M., Bowring S., Searle M., Waters D. and Hodges K.:Metamorphism, melting, and extension: age constraints from the High Himalayan slab of southeast Zaskar and northwest Lahaul, *The Journal of Geology*. 107, 473-495, 1999.
- Wan S., Li A., Clift P. D. and Stuu J.-B. W.:Development of the East Asian monsoon: Mineralogical and sedimentologic records in the northern South China Sea since 20 Ma, *Palaeogeography, Palaeoclimatology, Palaeoecology*. 254, 561-582, 2007.
- Wan S., Kürschner W. M., Clift P. D., Li A. and Li T.:Extreme weathering/erosion during the Miocene Climatic Optimum: Evidence from sediment record in the South China Sea, *Geophysical Research Letters*. 36, 2009.
- Wang E., Wan J. and Liu J.:Late Cenozoic geological evolution of the foreland basin bordering the West Kunlun range in Pulu area: Constraints on timing of uplift of northern margin of the Tibetan Plateau, *Journal of Geophysical Research*. 108, 2003.
- Wang J., Hu X., Jansa L. and Huang Z.:Provenance of the Upper Cretaceous–Eocene Deep-Water Sandstones in Sangdanlin, Southern Tibet: Constraints on the Timing of Initial India-Asia Collision, *The Journal of Geology*. 119, 293-309, 2011.
- Wang Z. X., Liang M. Y., Sun Y. Q. and Dai G. W.:Cenozoic tectonic and geomorphic evolution of the Longxi region in northeastern Tibetan Plateau interpreted from detrital zircon, *Science China: Earth Sciences*. 60, 1-12, 2017.



- 1096 Wang C.-Y., Han W.-B., Wu J.-P., Lou H. and Chan W. W.:Crustal structure beneath the eastern margin of the
1097 Tibetan Plateau and its tectonic implications, *Journal of Geophysical Research*. 112, 2007.
- 1098 Wang Y., Zheng J., Zheng Y., Liu X. and Sun G.:Paleocene-Early Eocene uplift of the Altyn Tagh Mountain:
1099 Evidence from detrital zircon fission track analysis and seismic sections in the northwestern Qaidam basin,
1100 *Journal of Geophysical Research: Solid Earth*. 120, 8534-8550, 2015.
- 1101 Wang S., Wang C., Phillips R. J., Murphy M. A., Fang X. and Yue Y.:Displacement along the Karakoram fault,
1102 NW Himalaya, estimated from LA-ICP-MS U–Pb dating of offset geologic markers, *Earth and Planetary
1103 Science Letters*. 337-338, 156-163, 2012a.
- 1104 Wang E., Kirby E., Furlong K. P., van Soest M., Xu G., Shi X., Kamp P. J. J. and Hodges K. V.:Two-phase growth
1105 of high topography in eastern Tibet during the Cenozoic, *Nature Geoscience*. 5, 640-645, 2012b.
- 1106 Wang W., Zhang P., Pang J., Garzzone C., Zhang H., Liu C., Zheng D., Zheng W. and Yu J.:The Cenozoic growth
1107 of the Qilian Shan in the northeastern Tibetan Plateau: A sedimentary archive from the Jiuxi Basin, *Journal
1108 of Geophysical Research: Solid Earth*. 121, 2235-2257, 2016a.
- 1109 Wang W., Zhang P., Liu C., Zheng D., Yu J., Zheng W., Wang Y., Zhang H. and Chen X.:Pulsed growth of the West
1110 Qinling at ~30 Ma in northeastern Tibet: Evidence from Lanzhou Basin magnetostratigraphy and provenance,
1111 *Journal of Geophysical Research: Solid Earth*. 121, 7754-7774, 2016b.
- 1112 Wang Q., Wyman D. A., Li Z.-X., Sun W., Chung S.-L., Vasconcelos P. M., Zhang Q., Dong H., Yu Y. and Pearson
1113 N.:Eocene north–south trending dikes in central Tibet: New constraints on the timing of east–west extension
1114 with implications for early plateau uplift?, *Earth and Planetary Science Letters*. 298, 205-216, 2010.
- 1115 Wang Q., Wyman D. A., Xu J., Dong Y., Vasconcelos P. M., Pearson N., Wan Y., Dong H., Li C., Yu Y., Zhu T.,
1116 Feng X., Zhang Q., Zi F. and Chu Z.:Eocene melting of subducting continental crust and early uplifting of
1117 central Tibet: Evidence from central-western Qiangtang high-K calc-alkaline andesites, dacites and rhyolites,
1118 *Earth and Planetary Science Letters*. 272, 158-171, 2008.
- 1119 Wei Y., Zhang K. X., Ji J. L., Song B. W., Jiang S. S. and Ke X.:Cenozoic sedimentation rate evolution of the
1120 Qaidam Basin in the Tibetan Plateau and its response to the uplift of the plateau [in chinese with English
1121 abstract], *Geol, Bull, China*. 32, 105-110, 2013.
- 1122 Westerhold T., Bickert T. and Röhl U.:Middle to late Miocene oxygen isotope stratigraphy of ODP site 1085 (SE
1123 Atlantic): new constrains on Miocene climate variability and sea-level fluctuations, *Palaeogeography,
1124 Palaeoclimatology, Palaeoecology*. 217, 205-222, 2005.
- 1125 Wiesmayr G. and Grasemann B.:Eohimalayan fold and thrust belt: Implications for the geodynamic evolution of
1126 the NW - Himalaya (India), *Tectonics*. 21, 2002.
- 1127 Willenbring J. K. and von Blanckenburg F.:Long-term stability of global erosion rates and weathering during late-
1128 Cenozoic cooling, *Nature*. 465, 211-214, 2010.
- 1129 Wu G., Liu Y., He B., Bao Q., Duan A. and Jin F. F.:Thermal controls on the Asian summer monsoon, *Sci Rep*. 2,
1130 404, 2012.
- 1131 Xiao G., Guo Z., Dupont-Nivet G., Lu H., Wu N., Ge J., Hao Q., Peng S., Li F., Abels H. A. and Zhang
1132 K.:Evidence for northeastern Tibetan Plateau uplift between 25 and 20Ma in the sedimentary archive of the
1133 Xining Basin, Northwestern China, *Earth and Planetary Science Letters*. 317-318, 185-195, 2012.



- 1134 Xu Q., Ding L., Zhang L., Cai F., Lai Q., Yang D. and Liu-Zeng J.:Paleogene high elevations in the Qiangtang
1135 Terrane, central Tibetan Plateau, Earth and Planetary Science Letters. 362, 31-42, 2013.
- 1136 Xu Y., Yue L., Li J., Sun L., Sun B., Zhang J., Ma J. and Wang J.:An 11-Ma-old red clay sequence on the Eastern
1137 Chinese Loess Plateau, Palaeogeography, Palaeoclimatology, Palaeoecology. 284, 383-391, 2009.
- 1138 Yan M., VanderVoo R., Fang X.-m., Parés J. M. and Rea D. K.:Paleomagnetic evidence for a mid-Miocene
1139 clockwise rotation of about 25° of the Guide Basin area in NE Tibet, Earth and Planetary Science Letters.
1140 241, 234-247, 2006.
- 1141 Yin A. and Harrison T. M.:Geologic evolution of the Himalayan-Tibetan orogen, Annual Review of Earth and
1142 Planetary Sciences. 28, 211-280, 2000.
- 1143 Yin A., Dang Y. Q., Zhang M., Chen X. H. and McRivette M. W.:Cenozoic tectonic evolution of the Qaidam basin
1144 and its surrounding regions (Part 3): Structural geology, sedimentation, and regional tectonic reconstruction,
1145 Geological Society of America Bulletin. 120, 847-876, 2008a.
- 1146 Yin A., Harrison T. M., Ryerson F., Wenji C., Kidd W. and Copeland P.:Tertiary structural evolution of the
1147 Gangdese thrust system, southeastern Tibet, Journal of Geophysical Research: Solid Earth. 99, 18175-18201,
1148 1994.
- 1149 Yin A., Nie S., Craig P., Harrison T., Ryerson F., Xianglin Q. and Geng Y.:Late Cenozoic tectonic evolution of the
1150 southern Chinese Tian Shan, Tectonics. 17, 1-27, 1998.
- 1151 Yin A., Dang Y.-Q., Wang L.-C., Jiang W.-M., Zhou S.-P., Chen X.-H., Gehrels G. E. and McRivette M.
1152 W.:Cenozoic tectonic evolution of Qaidam basin and its surrounding regions (Part 1): The southern Qilian
1153 Shan-Nan Shan thrust belt and northern Qaidam basin, Geological Society of America Bulletin. 120, 813-
1154 846, 2008b.
- 1155 Yin A., Rumelhart P., Butler R., Cowgill E., Harrison T., Foster D., Ingersoll R., Qing Z., Xian-Qiang Z. and Xiao-
1156 Feng W.:Tectonic history of the Altyn Tagh fault system in northern Tibet inferred from Cenozoic
1157 sedimentation, Geological Society of America Bulletin. 114, 1257-1295, 2002.
- 1158 Zachos J. C., Dickens G. R. and Zeebe R. E.:An early Cenozoic perspective on greenhouse warming and carbon-
1159 cycle dynamics, Nature. 451, 279-283, 2008.
- 1160 Zachos J. C., Shackleton N. J., Revenaugh J. S., Pälike H. and Flower B. P.:Climate response to orbital forcing
1161 across the Oligocene-Miocene boundary, Science. 292, 274-278, 2001.
- 1162 Zhang Z. S., Huijun W., Zhengtang G. and Dabang J.:What triggers the transition of palaeoenvironmental patterns
1163 in China, the Tibetan Plateau uplift or the Paratethys Sea retreat?, Palaeogeography, Palaeoclimatology,
1164 Palaeoecology. 245, 317-331, 2007.
- 1165 Zhang R., Jiang D., Liu X. and Tian Z.:Modeling the climate effects of different subregional uplifts within the
1166 Himalaya-Tibetan Plateau on Asian summer monsoon evolution, Chinese Science Bulletin. 57, 4617-4626,
1167 2012.
- 1168 Zhang R., Jiang D., Zhang Z., Cheng Z. and Zhang Q.:Comparison of the climate effects of surface uplifts from
1169 the northern Tibetan Plateau, the Tianshan, and the Mongolian Plateau on the East Asian climate, Journal of
1170 Geophysical Research Atmospheres. 122, 7949-7970, 2017.
- 1171 Zhang Y., Sun D., Li Z., Wang F., Wang X., Li B., Guo F. and Wu S.:Cenozoic record of aeolian sediment



- 1172 accumulation and aridification from Lanzhou, China, driven by Tibetan Plateau uplift and global climate,
1173 Global and Planetary Change. 120, 1-15, 2014.
- 1174 Zhang P.-Z., Shen Z., Wang M., Gan W., Bürgmann R., Molnar P., Wang Q., Niu Z., Sun J., Wu J., Hanrong S. and
1175 Xinzhaoy Y.:Continuous deformation of the Tibetan Plateau from global positioning system data, *Geology*. 32,
1176 809-812, 2004.
- 1177 Zhang K., Wang G., Ji J., Luo M., Kou X., Wang Y., Xu Y., Chen F., Chen R., Song B., Zhang J. and Liang
1178 Y.:Paleogene-Neogene stratigraphic realm and sedimentary sequence of the Qinghai-Tibet Plateau and their
1179 response to uplift of the plateau, *Science China Earth Sciences*. 53, 1271-1294, 2010.
- 1180 Zheng D., Clark M. K., Zhang P., Zheng W. and Farley K. A.:Erosion, fault initiation and topographic growth of
1181 the North Qilian Shan (northern Tibetan Plateau), *Geosphere*. 6, 937-941, 2010.
- 1182 Zheng H., Wei X., Tada R., Clift P. D., Wang B., Jourdan F., Wang P. and He M.:Late Oligocene-early Miocene
1183 birth of the Taklimakan Desert, *Proc Natl Acad Sci U S A*. 112, 7662-7668, 2015.
- 1184 Zheng D., Zhang P.-Z., Wan J., Yuan D., Li C., Yin G., Zhang G., Wang Z., Min W. and Chen J.:Rapid exhumation
1185 at ~8 Ma on the Liupan Shan thrust fault from apatite fission-track thermochronology: Implications for
1186 growth of the northeastern Tibetan Plateau margin, *Earth and Planetary Science Letters*. 248, 198-208, 2006.
- 1187 Zhu B., Kidd W. S., Rowley D. B., Currie B. S. and Shafique N.:Age of initiation of the India - Asia collision in
1188 the east - central Himalaya, *The Journal of Geology*. 113, 265-285, 2005.
- 1189 Zhu D.-C., Zhao Z.-D., Niu Y., Dilek Y., Hou Z.-Q. and Mo X.-X.:The origin and pre-Cenozoic evolution of the
1190 Tibetan Plateau, *Gondwana Research*. 23, 1429-1454, 2013.
- 1191 Zhu D. C., Wang Q., Zhao Z. D., Chung S. L., Cawood P. A., Niu Y., Liu S. A., Wu F. Y. and Mo X. X.:Magmatic
1192 record of India-Asia collision, *Sci Rep*. 5, 14289, 2015.
- 1193 Zhuang G., Pagani M. and Zhang Y. G.:Monsoonal upwelling in the western Arabian Sea since the middle
1194 Miocene, *Geology*. 45, 655-658, 2017.
- 1195 Zhuang G., Hourigan J. K., Koch P. L., Ritts B. D. and Kent-Corson M. L.:Isotopic constraints on intensified
1196 aridity in Central Asia around 12Ma, *Earth and Planetary Science Letters*. 312, 152-163, 2011.
- 1197 Ziegler C. L., Murray R. W., Hovan S. A. and Rea D. K.:Resolving eolian, volcanogenic, and authigenic
1198 components in pelagic sediment from the Pacific Ocean, *Earth and Planetary Science Letters*. 254, 416-432,
1199 2007.

1200

1201 Figure captions

1202 Fig 1. Major tectonic units of the Himalayan-Tibetan orogen and its movements constrained by global positioning
1203 system measurements. The global positioning system velocities in and around the Tibetan Plateau with respect to
1204 stable Eurasia are from Zhang et al. (2004). Abbreviations: IYS-Indus-Yarlung suture; JF: Jiali fault; BNS:
1205 Bangong-Nujiang suture; JS: Jinsha suture; XF:Xianshuihe fault; KLF: Karakomrum fault; KS: Karakash fault; KF:
1206 Kunlun fault; ALT: Altyn Tagh fault.

1207

1208 Fig 2. Topographic map of the Tibetan Plateau showing evidence of rejuvenation or initiation of tectonic activities
1209 at ~65-35 Ma. The black circles represent some geographic locations mentioned in the article. The detailed



1210 information of tectonic activities at ~65–35 Ma is shown in table 1.

1211

1212 Fig 3. Temporal evolution of paleoclimatic proxies over the time period 26–20 Ma. (A) long-term variations of
1213 eccentricity (Laskar et al., 2004); (B) the reconstruction atmospheric CO₂ based on di-unsaturated alkenones
1214 (Pagani et al., 1999a, 1999b, 2005); (C) Benthic foraminiferal carbon isotope from ODP site 1218 in Pacific
1215 (Pälike et al., 2006); (D) Benthic foraminiferal oxygen isotope from ODP site 1218; (E) Sea-level estimates from
1216 the New Jersey and Delaware coastal plain coreholes (Kominz et al., 2008), with best estimates (black circles) and
1217 best with imaginary lowstands (green circles); (F) Carbonate content estimated by In (Ca/Fe) from ODP 1264
1218 (black line) and 1265 (red line) in the subtropical southeastern Atlantic Ocean (Liebrand et al., 2016); (G) Weight
1219 percent (wt%) records of >150 µm size fractions from ODP 1264 in the subtropical southeastern Atlantic Ocean
1220 (Liebrand et al., 2016); (H) Benthic foraminiferal accumulation rates (blue curve) and benthic foraminiferal tests
1221 per gram sediment (pink curve) from ODP site 1090 in the southern Atlantic Ocean (Diester-Haass et al., 2011).

1222

1223 Fig 4. Topographic map of the Tibetan Plateau showing evidence of rejuvenation or initiation of tectonic activities
1224 at 30–20 Ma. The black circles represent some geographic locations mentioned in the article. The detailed
1225 information of tectonic activities at 30–20 Ma is shown in table.2.

1226

1227 Fig 5. Temporal evolution of paleoclimatic proxies over the time period 16–8 Ma. (A) long-term variations of
1228 eccentricity (Laskar et al., 2004); (B) reconstruction of atmospheric CO₂ from di-unsaturated alkenones with
1229 uncertainty band (Pagani et al., 1999a, 1999b, 2005) (yellow circles) and boron isotope data with uncertainty band
1230 (Foster et al., 2012) (blue circles), and from B/Ca (Tripathi et al., 2009); (C) and (D) Benthic foraminiferal oxygen
1231 and carbon isotope from ODP Site 1146 in South China Sea (Holbourn et al., 2007, 2013); (E) Sea-level estimates
1232 from the New Jersey and Delaware coastal plain coreholes (Kominz et al., 2008), with best estimates (red circles)
1233 and best with imaginary lowstands (blue circles); (F) Sea Surface Temperature (SST) estimated by Rousselle et
1234 al. (2013) from IODP site U1338 in the Eastern Equatorial Pacific; (G) Mass accumulation rates (MAR) of silicate
1235 sediments at ODP site 1146 (red boxes) (Wan et al., 2009) and ODP site 1148 (black circles) (Clift, 2006).

1236

1237 Fig 6. Temporal evolution of paleoclimatic proxies over the time period 16–8 Ma in Asia. (A) pollen grains of
1238 *Chenopodiaceae* from Sikouzi section in the east side of the Liupan Mountains (green) (Jiang and Ding, 2008) and
1239 from western Qaidam basin (pink) (Miao et al., 2013); (B) Pedogenic and lacustrine carbonates δ¹⁸O from
1240 northeastern Qaidam basin (black circles) (Zhuang et al., 2011) and Xunhua basin in the northeastern Tibetan
1241 Plateau (red circles) (Hough et al., 2011); (C) illite/smectite ratios from IODP U1430 in Japan Sea (Shen et al.,
1242 2017); (D) carbonate contents from Qaidam basin (Song et al., 2014); (E) the CIA (100×Al₂O₃/(Al₂O₃+CaO+
1243 Na₂O+K₂O)) from ODP 1146 in the South China Sea (Wan et al., 2009); (F) Magnetic susceptibility from the
1244 Zhuanglang section in the western Loess Plateau (Qiang et al., 2011); (G) Mn/Ca ratios of a 3 point running
1245 average from IODP site U1466, U1468 and U1471 in Indian Ocean (Betzler et al., 2016); (F) total organic carbon
1246 (TOC wt%) values from ODP site 731A and 722B in the western Arabian Sea (Gupta et al., 2015).

1247



Fig. 7. Topographic map of the Tibetan Plateau showing evidence of rejuvenation or initiation of tectonic activities during 15-8 Ma. The black circles represent some geographic locations mentioned in the article. The detailed information of tectonic activities during 15-8 Ma is shown in table.3.

Fig 8. Evolution of Asian climate and the Tibetan Plateau, and their relation with global changes during the Cenozoic. The data of benthic foraminiferal $\delta^{18}\text{O}$ and atmospheric CO_2 content is modified from Zachos et al. (2001) and Zachos et al. (2008), respectively.

Figure 1

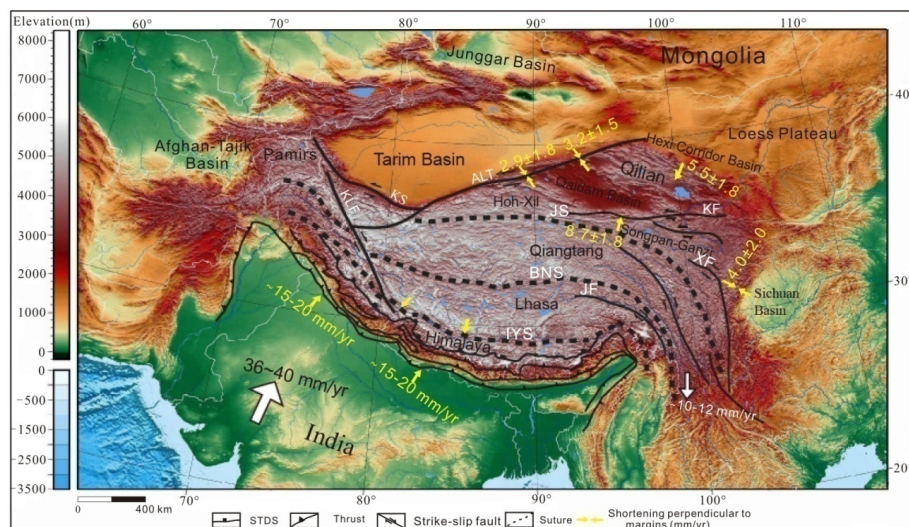
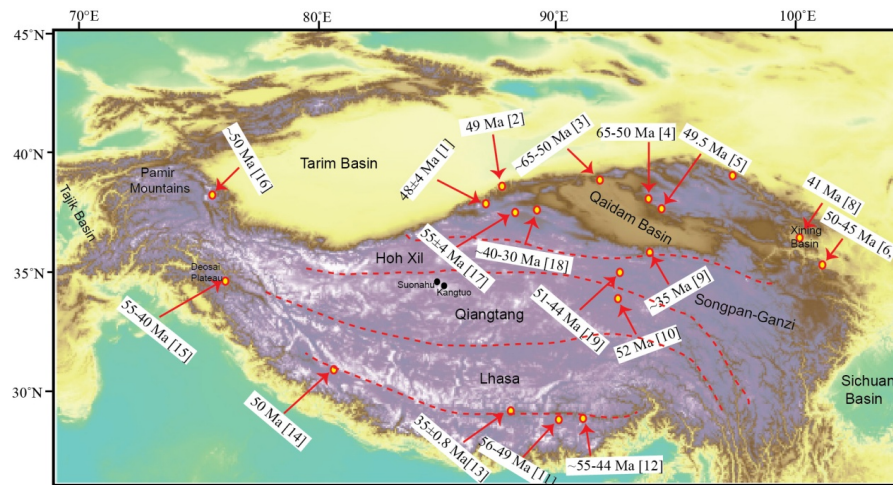
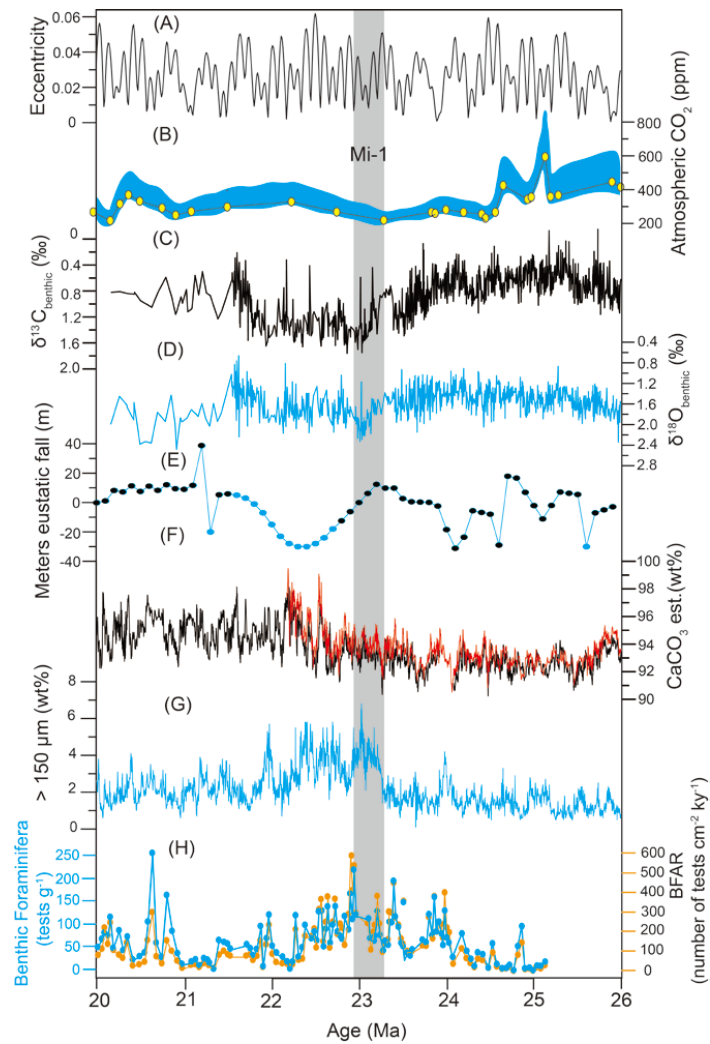


Figure 2

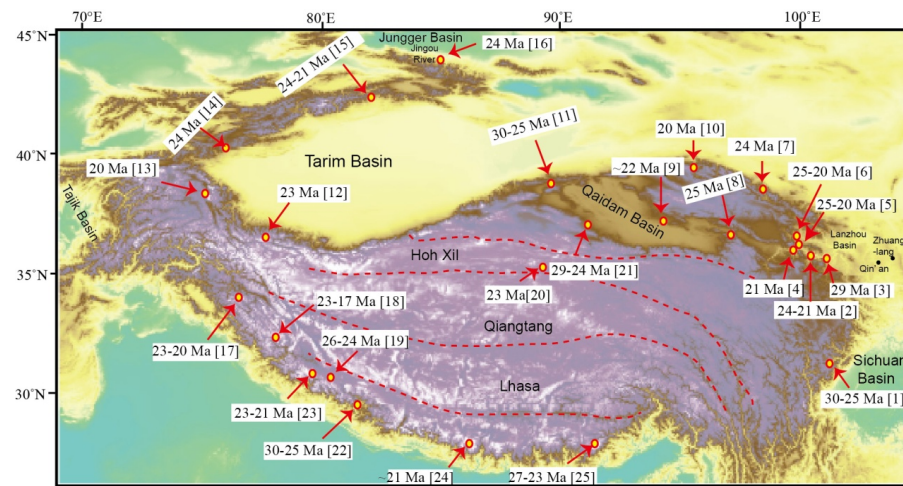


1299 Figure 3
1300

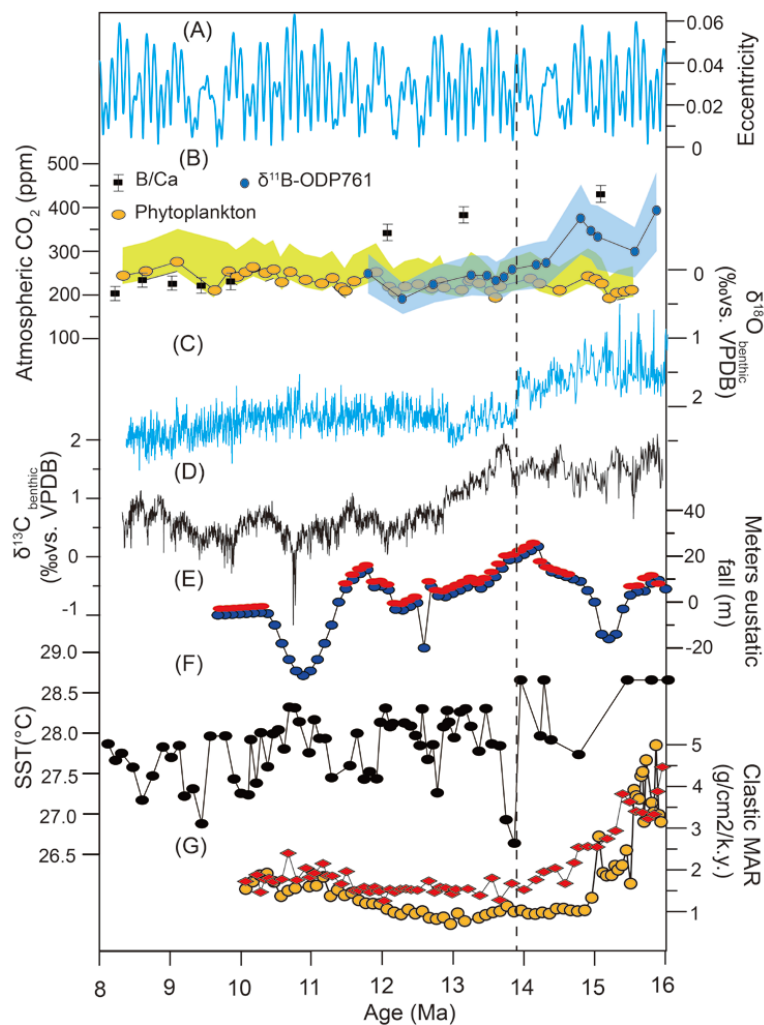


1301
1302
1303
1304
1305
1306
1307
1308
1309
1310

Figure 4

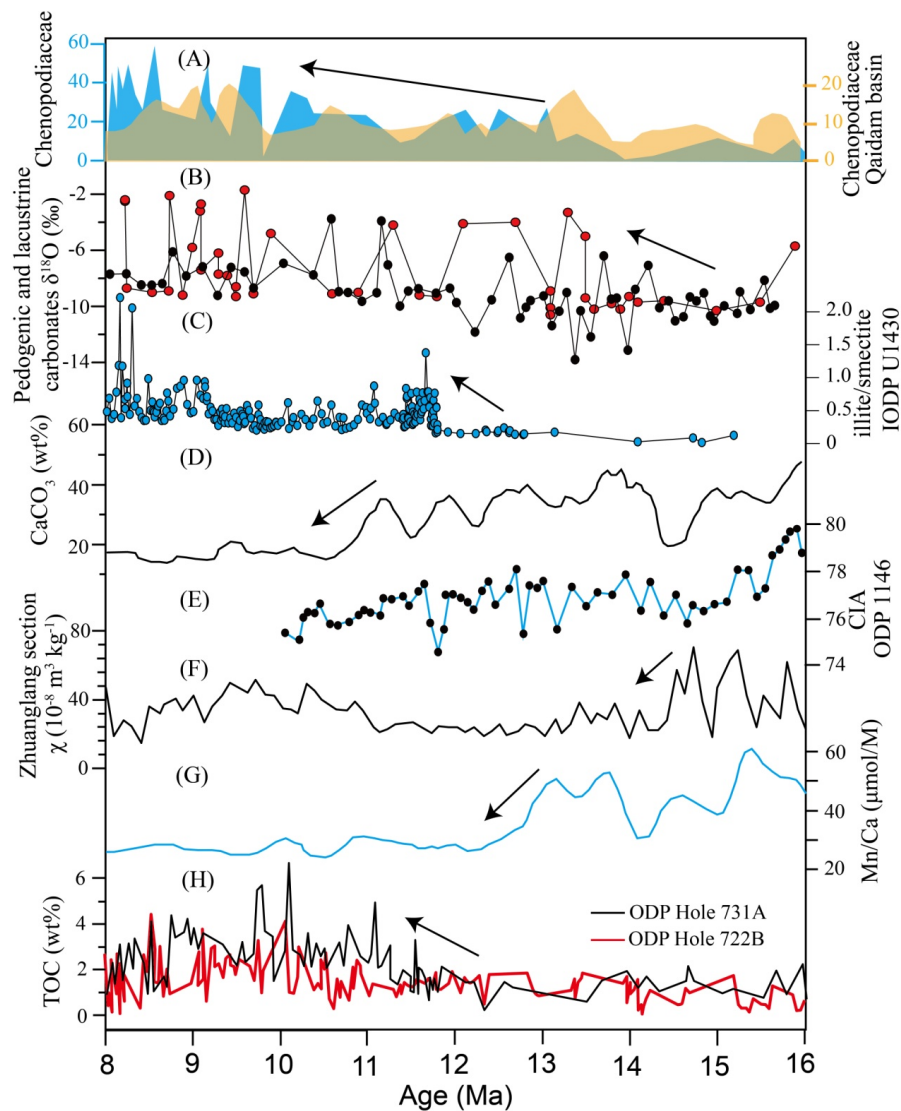


1337 Figure 5



1338
 1339
 1340
 1341
 1342
 1343
 1344
 1345
 1346
 1347
 1348

1349 Figure 6



1350
1351
1352
1353
1354
1355
1356
1357
1358



Figure 7

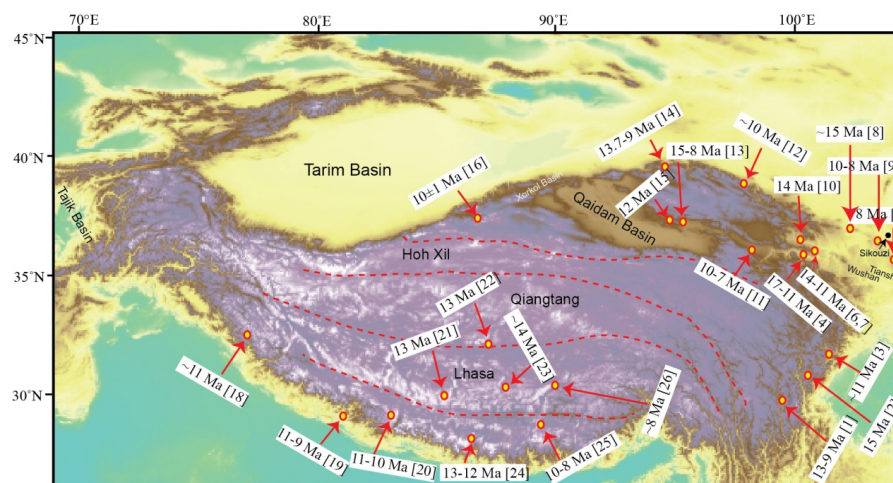


Figure 8

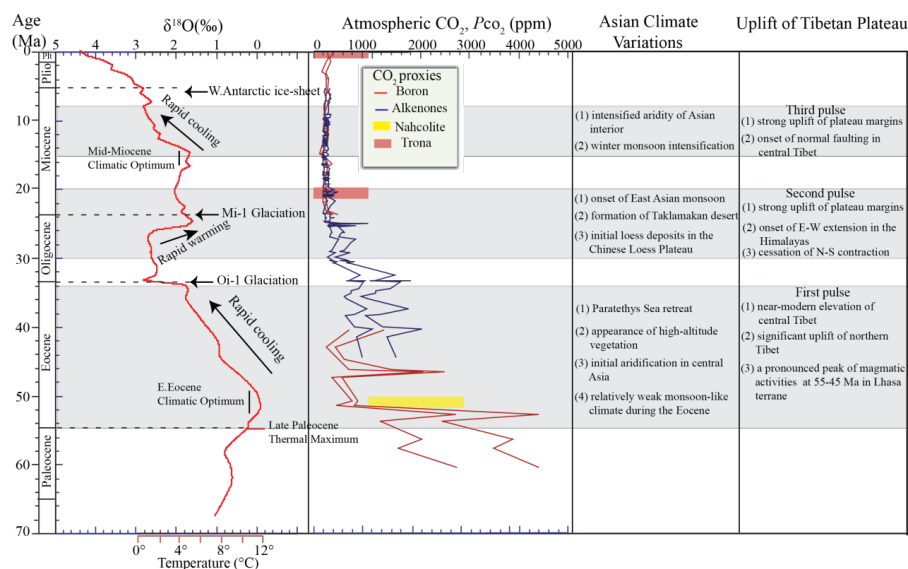


Table captions

Table 1. Detailed information of rejuvenation or initiation of tectonic activities at ~65-35 Ma in the Tibetan Plateau.



1370

1371 Table 2. Detailed information of rejuvenation or initiation of tectonic activities at 30-

1372 20 Ma in the Tibetan Plateau.

1373

1374 Table 3. Detailed information of rejuvenation or initiation of tectonic activities at 15-8

1375 Ma in the Tibetan Plateau.

1376

1377 Table 1

Region/thrusts	Events and Ages	Methods	References	Marks
Altyn Tagh fault	Initial active (~49 Ma)	Apatite fission track (AFT)	Jolivet et al. (2001), Yin et al. (2002)	[1,2]
Altyn Tagh	Rapid uplift (65-50 Ma)	Zircon fission track and sedimentary	Wang et al. (2015)	[3]
Northern Qaidam basin	Initial contraction (65-50 Ma)	Seismic reflection and balanced cross section	Yin et al. (2008a)	[4]
Northern Qaidam basin	High accumulation rate (~49.5 Ma)	Sediments	Wei et al. (2013)	[5]
West Qinling thrust	Rapid cooling (50-45 Ma)	Apatite (U-Th)/He	Clark et al. (2010)	[6]
West Qinling thrust	Initial active (~50 Ma)	^{40}Ar - ^{39}Ar	Duvall et al. (2011)	[7]
Xining basin	25° of clockwise rotation (41 Ma)	Paleomagnetic data	Dupont-Nivet et al. (2008b)	[8]
Eastern Kunlun	Rapid cooling (~35 Ma)	Apatite (U-Th)/He	Clark et al. (2010)	[9]
Tanggula thrust	Initial active (~52 Ma)	Sediments and angular unconformities	Li et al. (2012)	[10]
Tethyan Himalaya thrust	Initial active (56-49 Ma)	^{40}Ar - ^{39}Ar	Wiesmayr and Grasemann (2002)	[11]
Tethyan Himalayan	Significant crustal thickening (~55-44 Ma)	U-Pb, K-Ar and ^{40}Ar - ^{39}Ar	Aikman et al. (2008)	[12]
Mabja Dome	Onset of mid-crustal extension (35±0.8 Ma)	U-Pb	Lee and Whitehouse (2007)	[13]
Northwestern Himalaya	Large-scale granite intrusion (~50 Ma)	U-Pb	Wang et al. (2012a)	[14]
Deosai plateau	Rapid cooling (55-40 Ma)	AFT, apatite and zircon (U-Th)/He	van der Beek et al. (2009)	[15]
Kashgar-Yecheng thrust	Initial motion (~50 Ma)	zircon and apatite fission track	Cao et al. (2013)	[16]
Kunlun fault	Rapid cooling (55±4 Ma)	AFT	Jolivet et al. (2001)	[17]
Qimen Tagh mountains	Initial uplift (~40-30 Ma)	AFT	Liu et al. (2015b)	[18]
Fenghuoshan fold-thrust belt	Initial deformation (51-44 Ma)	AFT, apatite (U-Th)/He, ^{40}Ar - ^{39}Ar	Staisch et al. (2016)	[19]

1378



1379 Table 2

Region/thrust	Events and Ages	Method	Reference	Marks
Longmen Shan	Initial uplift (30-25 Ma)	AFT, apatite and zircon (U-Th)/He	Wang et al. (2012b)	[1]
Xunhua basin	High accumulation rates (24-21 Ma)	Magnetostratigraphy	Lease et al. (2012)	[2]
Linxia Basin	Rapid subsidence (29 Ma)	Magnetostratigraphy	Fang et al. (2003)	[3]
Guide Basin	Sedimentary discontinuity (21 Ma)	Structural geology and sedimentary	Liu et al. (2013)	[4]
Laji Shan	Rapid uplift (25-20 Ma)	Magnetostratigraphy and U-Pb	Lease et al. (2012)	[5]
Xining basin	Unstable accumulations (25-20 Ma)	Magnetostratigraphy	Xiao et al. (2012)	[6]
Northeast Qilian	Rapid cooling (24 Ma)	AFT	Pan et al. (2013)	[7]
Elashan	Rapid uplift (25 Ma)	Magnetostratigraphy and AFT	Lu et al. (2012)	[8]
North Qaidam basin	Fault reactivation (~22 Ma)	Constrained by the sedimentary	Lu and Xiong (2009)	[9]
North Qilian	Rapid exhumation (20 Ma)	AFT, vitrinite-reflectance analysis	George et al. (2001)	[10]
Altyn Tagh fault	Rapid exhumation (30-25 Ma)	AFT and sediments	Jolivet et al. (2001)	[11]
West Kunlun Shan	Rapid uplift (23 Ma)	Seismic reflection and drill-well data	Jiang et al. (2013)	[12]
Main Pamir thrust	Rapid cooling (20 Ma)	AFT	Sobel and Dumitru (1997)	[13]
Southwest Tian Shan	Rapid exhumation (24 Ma)	AFT	Sobel et al. (2006)	[14]
Southern Tian Shan	Initial uplift (24-21 Ma)	Sedimentary record and Magnetostratigraphy	Yin et al. (1998)	[15]
Northern Tian Shan	Initial unroofing (~24 Ma)	AFT	Hendrix et al. (1994)	[16]
Zaskar Shear Zone	Cooling ages of muscovites (23-20 Ma)	$^{40}\text{Ar}-^{39}\text{Ar}$	Walker et al. (1999)	[17]
Sutlej Rift	Exhumation of deep crustal rocks (23-17 Ma)	$^{40}\text{Ar}-^{39}\text{Ar}$	Vannay et al. (2004)	[18]
Kailas basin	Initial deposition (26-24 Ma)	Igneous zircon U-Pb age	DeCelles et al. (2011)	[19]
Hoh Xil basin	Sedimentary discontinuity (23 Ma)	Constrained by sedimentation	Wang et al. (2002)	[20]
Eastern Kunlun	Initial uplift (29-24 Ma)	Constrained by sedimentary of foreland basin	Yin et al. (2008b)	[21]
Ama Drime range	Partial melting (30-25 Ma)	(U-Th)/He, $^{40}\text{Ar}-^{39}\text{Ar}$ and U-Th/Pb	Kali et al. (2010)	[22]
Silving leucogranite	Rapid cooling (23-21 Ma)	U-Pb, AFT and $^{40}\text{Ar}-^{39}\text{Ar}$	Searle et al. (1999)	[23]
Everest	Initial movement of MCT (~21 Ma)	U-Pb and $^{40}\text{Ar}-^{39}\text{Ar}$	Viskopic et al. (2005)	[24]
Gangdese thrust	Initial motion (27-23 Ma)	$^{40}\text{Ar}-^{39}\text{Ar}$	Yin et al. (1994)	[25]

1380
1381
1382
1383
1384



1385 Table 3

Region/thrust	Events and Ages	Method	Method	Marks
Southeastern Tibet	Rapid cooling (13-9 Ma)	AFT and apatite (U-Th)/He	Clark et al. (2005b)	[1]
Southwestern Longmen	Rapid exhumation (15 Ma)	AFT, apatite and zircon (U-Th)/He	Cook et al. (2013)	[2]
Central Longmen Shan	Rapid exhumation (~11 Ma)	⁴⁰ Ar- ³⁹ Ar, apatite and zircon (U-Th)/He	Kirby et al. (2002)	[3]
Guide basin	Clockwise rotation (17-11 Ma)	Paleomagnetic data	Yan et al. (2006)	[4]
Liupan Shan	Rapid exhumation (~8 Ma)	AFT	Zheng et al. (2006)	[5]
Jishi Shan	Rapid uplift (14-11 Ma)	AFT, apatite (U-Th)/He and U-Pb	Lease et al. (2011,2012)	[6,7]
Central Haiyuan fault	Initial motion (~15 Ma)	AFT, apatite and zircon (U-Th)/He	Duvall et al. (2013)	[8]
Eastern Haiyuan fault	Initial motion (10-8 Ma)	AFT, apatite and zircon (U-Th)/He	Duvall et al. (2013)	[9]
Xining basin	Significant uplift (14 Ma)	Paleomagnetic age of river terraces	Lu et al. (2004)	[10]
Gonghe Nan Shan	Initial active (10-7 Ma)	Constrained by sediments of foreland basin	Craddock et al. (2011)	[11]
North Qilian Shan	Rapid cooling (~10 Ma)	Apatite (U-Th)/He	Zheng et al. (2010)	[12]
Eastern Qaidam basin	High accumulation rates (15-8 Ma)	Inferred from magnetostratigraphy	Fang et al. (2007)	[13]
Altyn Tagh	Rapid uplift (13.7-9 Ma)	Paleomagnetic age of molasse deposits	Sun et al. (2005)	[14]
Southern Qilian Shan	Rapid uplift (12 Ma)	Magnetostratigraphy	Lu and Xiong (2009)	[15]
Altyn Tagh fault	Rapid cooling (10±1 Ma)	AFT	Jolivet et al. (2001)	[16]
West Kunlun	Rapid uplift (12-8 Ma)	AFT	Wang et al. (2003)	[17]
Sutlej Valley	Peak metamorphism (~11 Ma)	U-Pb ages	Caddick et al. (2007)	[18]
Main Boundary thrust	Initial motion (11-9 Ma)	Inferred from sediments in Siwalik Group	Meigs et al. (1995)	[19]
Thakkola rift	Initial extension (11-10 Ma)	Magnetostratigraphy	Garzione et al. (2000)	[20]
Tangra Yumco rift	Initial extension (13-12 Ma)	Zircon and apatite (U-Th)/He	Dewane et al. (2006)	[21]
Shuanghu rift	Initial extension (13 Ma)	⁴⁰ Ar- ³⁹ Ar	Blisniuk et al. (2001)	[22]
Xainza rift	Initial extension (~14 Ma)	U-Pb and apatite (U-Th)/He	Hager et al. (2009)	[23]
Kung Co rift	Initial extension (13-12 Ma)	Zircon and apatite (U-Th)/He	Lee et al. (2011)	[24]
Yadong-Gulu rift	Initial extension (10-8 Ma)	Constrained by monazite Th-Pb ages	Edwards and Harrison (1997)	[25]
Nyainqentanglha rift	Initial extension (~8 Ma)	⁴⁰ Ar- ³⁹ Ar	Harrison et al. (1995)	[26]